



HAL
open science

Assessing the effects of earlier snow melt-out on Alpine shrub growth: the sooner the better?

L. Francon, Thierry Ameglio, Christophe Corona, I. Till-Bottraud, P. Choler, B.Z. Carlson, Guillaume Charrier, Samuel Morin, Nicolas Eckert, E. Roussel, et al.

► To cite this version:

L. Francon, Thierry Ameglio, Christophe Corona, I. Till-Bottraud, P. Choler, et al.. Assessing the effects of earlier snow melt-out on Alpine shrub growth: the sooner the better?. *Ecological Indicators*, 2020, 115, pp.106455. 10.1016/j.ecolind.2020.106455 . hal-02903838

HAL Id: hal-02903838

<https://hal.inrae.fr/hal-02903838v1>

Submitted on 21 Jul 2020

HAL is a multi-disciplinary open access archive for the deposit and dissemination of scientific research documents, whether they are published or not. The documents may come from teaching and research institutions in France or abroad, or from public or private research centers.

L'archive ouverte pluridisciplinaire **HAL**, est destinée au dépôt et à la diffusion de documents scientifiques de niveau recherche, publiés ou non, émanant des établissements d'enseignement et de recherche français ou étrangers, des laboratoires publics ou privés.

1 Assessing the effects of earlier snow melt-out on Alpine 2 shrub growth: the sooner the better?

3 L. Francon^{1*}, C. Corona¹, I. Till-Bottraud¹, P. Choler², B. Carlson³, G. Charrier^{4,5}, T.
4 Améglio^{4,5}, S. Morin⁶, N. Eckert⁷, E. Roussel¹, J. Lopez-Saez⁸, M. Stoffel^{8,9,10}

5
6 ¹Université Clermont Auvergne, CNRS, Geolab, F-63000 Clermont-Ferrand, France

7 ²Université Grenoble Alpes, Université Savoie Mont-Blanc, CNRS, LECA, F-38000 Grenoble, France

8 ³ Centre de Recherches sur les Ecosystèmes d'Altitude (CREA), Observatoire du Mont-Blanc, 74400
9 Chamonix, France

10 ⁴Université Clermont Auvergne, F-63000 Clermont-Ferrand, France

11 ⁵INRA, PIAF, F-63000 Clermont-Ferrand, France

12 ⁶Météo-France – CNRS, CNRM UMR 3589, Centre d'Études de la Neige, Grenoble, France

13 ⁷Université Grenoble Alpes, Irstea, UR ETGR, F-38000 Grenoble, France

14 ⁸Climate Change Impacts and Risks in the Anthropocene (C-CIA), Institute for Environmental Sciences,
15 University of Geneva, Geneva, Switzerland.

16 ⁹Department of Earth Sciences, University of Geneva, Geneva, Switzerland.

17 ¹⁰Department F.-A. Forel for Environmental and Aquatic Sciences, University of Geneva, Geneva,
18 Switzerland.

19 *Contact information: loic.francon@etu.uca.fr

21 Abstract

22 Enhanced shrub growth in a warming alpine climate has potential far-reaching implications,
23 including soil nutrient cycling, carbon storage, or water and surface energy exchanges. Growth
24 ring analysis can yield mid- to long-term, annually resolved records of shrub growth, and
25 thereby offer valuable insights into how growth is driven by interannual climate variability. In
26 the European Alps, dendroecological approaches have shown that dwarf shrub productivity is
27 influenced by interannual variations of growing season temperature but results also point to a
28 negative effect of winter precipitation on radial growth. However, as past work lacked snow
29 cover data, links between snow cover duration, growing season length, energy availability and
30 inter-annual shrub growth remain poorly understood.

31 In this paper, we combined multi-decadal shrub-ring series from 49 individuals sampled at three
32 sites along a 600-m elevational gradient in the Taillefer massif, located in the French Alps to
33 assess growth sensitivity of long-lived and widespread *Rhododendron ferrugineum* shrubs to

34 both snow cover dynamics and temperature changes. To this end, we computed structural
35 equation models to track the response of shrub radial growth to extending growing season at
36 1800, 2000 and 2400 m above sea level and for two time periods (i.e. 1959-1988 and 1989-
37 2016). The second period is marked by a significant advance in snow melt-out resulting in a
38 regime shift highlighted at the end of the 1980s by a breakpoint analysis.

39 At the high-elevation site, our results demonstrate a positive effect of increasing growing season
40 length on shrub growth, which is strongly dependent on snowpack depth and snow cover
41 duration. Conversely, at lower elevations, earlier melt-out dates and associated late frost
42 exposure are shown to lead to radial growth reduction. Moreover, the climate signal in ring-
43 width chronologies of *R. ferrugineum* portrays a weakening since 1988 – similar to a
44 phenomenon observed in series from circumpolar and alpine tree-ring sites and referred to as
45 “divergence”.

46 By analyzing long-term records of radial growth along an elevation gradient, our work provides
47 novel insights into the complex responses of shrub growth to climate change in alpine
48 environments. This paper demonstrates that *R. ferrugineum*, as a dominant alpine shrub species,
49 behave as an ecological indicator of the response of alpine ecosystem to global warming.

50 **Keywords**

51 dendrochronology; dendroecology; shrub expansion; dwarf shrubs; *Rhododendron*
52 *ferrugineum*; Structural Equation Model; divergence; elevation gradient; frost; snow cover
53

54 **Introduction**

55 Temperatures in Arctic and Alpine regions have been increasing twice as fast as the global
56 average over the last decades (Stocker et al., 2013), with potential far-reaching consequences
57 for ecosystem functioning due to feedbacks between vegetation and climate (Bjorkman et al.,
58 2018, 2020; Pearson et al., 2013). Rapid climate warming is also driving changes in the
59 structure and composition of cold ecosystems and has been associated with changes in plant

60 phenology, diversity and richness (Boscutti et al., 2018; Grabherr et al., 1994; Myers-Smith et
61 al., 2019; Steinbauer et al., 2018), poleward and upslope shifts in species geographic
62 distribution (Chen et al., 2011; Elsen and Tingley, 2015; Lenoir et al., 2008; Parmesan and
63 Yohe, 2003; Walther et al., 2002) and thermophilization (Dolezal et al., 2016; Elmendorf et al.,
64 2015; Gottfried et al., 2012). At high-latitude sites, increasing vegetation productivity (Pearson
65 et al., 2013) associated with a widespread shrub expansion (Elmendorf et al., 2015; Sturm et
66 al., 2001; Tape et al., 2006) has resulted in a greening trend, characterized by increasing canopy
67 cover, height, abundance, and biomass (Forbes et al., 2010; Hollesen et al., 2015; Myers-Smith
68 et al., 2011, 2015a, 2020). Conversion of tundra to shrubland is driven by ongoing warming,
69 and modulated by soil moisture (Ackerman et al., 2017; Elmendorf et al., 2012), but also by
70 changes in snow cover duration (Gamm et al., 2018; Niittynen et al., 2018; Weijers et al., 2018a;
71 Young et al., 2016). Recent warming and related shrubification (i.e. increasing shrub cover and
72 biomass) in Arctic systems has also been shown to drive climate feedbacks, for instance by
73 altering surface albedo, energy, water balance, or permafrost (Blok et al., 2011; Chapin, 2005;
74 Liston et al., 2002; Sturm et al., 2001). Although comparable changes can be expected at high
75 altitudes, shrubification has hitherto received very little consideration in temperate mountain
76 systems.

77 In the European Alps, documentation of upslope advancement of shrub species remains scarce
78 and spatially limited (Anthelme et al., 2007; Cannone et al., 2007; Dullinger et al., 2003;
79 Malfasi and Cannone, 2020). At the regional scale, Carlson et al., (2017) provided remote
80 sensing-based evidence linking the observed greening of alpine vegetation (increased
81 productivity) to increasing air temperatures and decreasing snow cover duration. Snow
82 manipulation experiments, designed to simulate the expected advance of melt-out dates in a
83 warmer climate (Gerdol et al., 2013; Rixen et al., 2010; Wipf and Rixen, 2010) confirm the
84 strong control of snowpack duration on shrub phenology and growth via indirect effects on soil

85 temperature, nutrient availability and frost exposure. Despite the indisputable value of these
86 studies to improve understanding of climate–growth linkages, experimental studies typically
87 cover relatively short periods (1-2 years; Wipf and Rixen, 2010) and cannot capture longer-
88 term shrub growth responses to climate change.

89 By contrast, growth-ring analyses have the potential to provide uninterrupted mid- to long-term,
90 annually-resolved records of shrub growth, thereby revealing responses to interannual climate
91 variability (Bär et al., 2006; Buchwal et al., 2013; Forbes et al., 2010; Hantemirov et al., 2000;
92 Hollesen et al., 2015; Weijers et al., 2010; Young et al., 2016 and Myers-Smith et al., 2015b
93 for an exhaustive review). Still underused in high-altitude environments, the limited number of
94 existing dendroecological studies tends to confirm that dwarf shrub productivity is influenced
95 by interannual variations of growing season temperature (Francon et al., 2017; Franklin, 2013;
96 Liang et al., 2012; Liang and Eckstein, 2009; Lu et al., 2015; Pellizzari et al., 2014). In the
97 Alps, initial results point to a negative effect of winter precipitation on the radial growth of
98 shrubs (Carrer et al., 2019; Francon et al., 2017; Pellizzari et al., 2014; Rixen et al., 2010), a
99 phenomenon that has been observed only rarely in circum-Arctic tundra ecosystems (Bär et al.,
100 2008; Hallinger et al., 2010; Ropars et al., 2015; Zalatan and Gajewski, 2006; but see Schmidt
101 et al., 2010, who found snow to correlate negatively with *Salix arctica* growth). Several
102 hypotheses have been proposed to explain this phenomenon, such as the detrimental effect of
103 late-persisting snow on the onset of cambial activity, growing season length or soil temperatures
104 (Pellizzari et al., 2014). In the Alps, the positive effects of longer and warmer growing seasons
105 could be offset by the negative effect of increased late-frost exposure due to earlier melt-out
106 dates (Jonas et al., 2008; Rixen et al., 2012). Most of the previous dendroecological studies,
107 however, relied on monthly-resolved meteorological time series and lacked snow cover data,
108 thereby precluding a precise assessment of the relationships between snow cover duration,
109 growing season length and energy availability during the snow free period. In addition, in the

110 Alps, existing dendroecological studies addressing the sensitivity of shrubs to climate have
111 largely ignored the role of topography, and even more so changes along elevational gradients.
112 We argue that by ignoring the impact of changes in snow cover alongside temperature at
113 different elevations, shrub ring–climate studies focusing on plant growth in temperate mountain
114 ecosystems will likely dismiss an obvious mechanistic pathway, which could potentially
115 regulate shrub growth in response to winter snow accumulation. This knowledge gap is
116 particularly pressing given the wealth of studies documenting a warming-induced decrease of
117 snow cover duration in temperate alpine regions of North America (Mote et al., 2005) and
118 Europe (Beniston et al., 2018; Hantel et al., 2000, 2012; López-Moreno, 2005). Ongoing and
119 future climate change will likely accelerate warming, but also favor earlier melt-out dates and
120 decreased snowpack depths at altitudes comprised between 1500 and 3000 m above sea level
121 (asl; Beniston et al., 2018; Marty et al., 2017; Steger et al., 2013; Verfaillie et al., 2018).

122 Here, we investigate long-term relationships between snow cover dynamics and the growth of
123 *Rhododendron ferrugineum* in the Taillefer massif where shrub growth is expected to be
124 influenced by snow cover dynamics (Francon et al., 2017) and where plants are likely to be
125 vulnerable to climate change. We use individuals sampled at three sites along a 600-m
126 elevational gradient. In order to test the hypothesis that shrub growth is directly positively
127 influenced by the accumulation of degree days received after the snow melt-out date (SFGDD),
128 we (i) developed multidecadal shrub-ring series from long-lived *Rhododendron ferrugineum*
129 individuals; (ii) evaluated recent climatic trends in atmospheric temperature, snow cover and
130 SFGDD obtained from a locally calibrated meteorological model, specifically designed for the
131 mountain environment and spanning the period 1958-2016 (Durand et al., 2009a, 2009b) and
132 (iii) investigate climate–growth relationships using structural equation models (SEMs)
133 designed to disentangle the effects of the above-mentioned climate variables on radial growth.

134 We computed SEMs for the periods 1959-1988 and 1989-2016 to test for the potential change
135 in shrub sensitivity to climatic drivers in the context of recent climate changes.

136

137 **Material and methods**

138 *Study species*

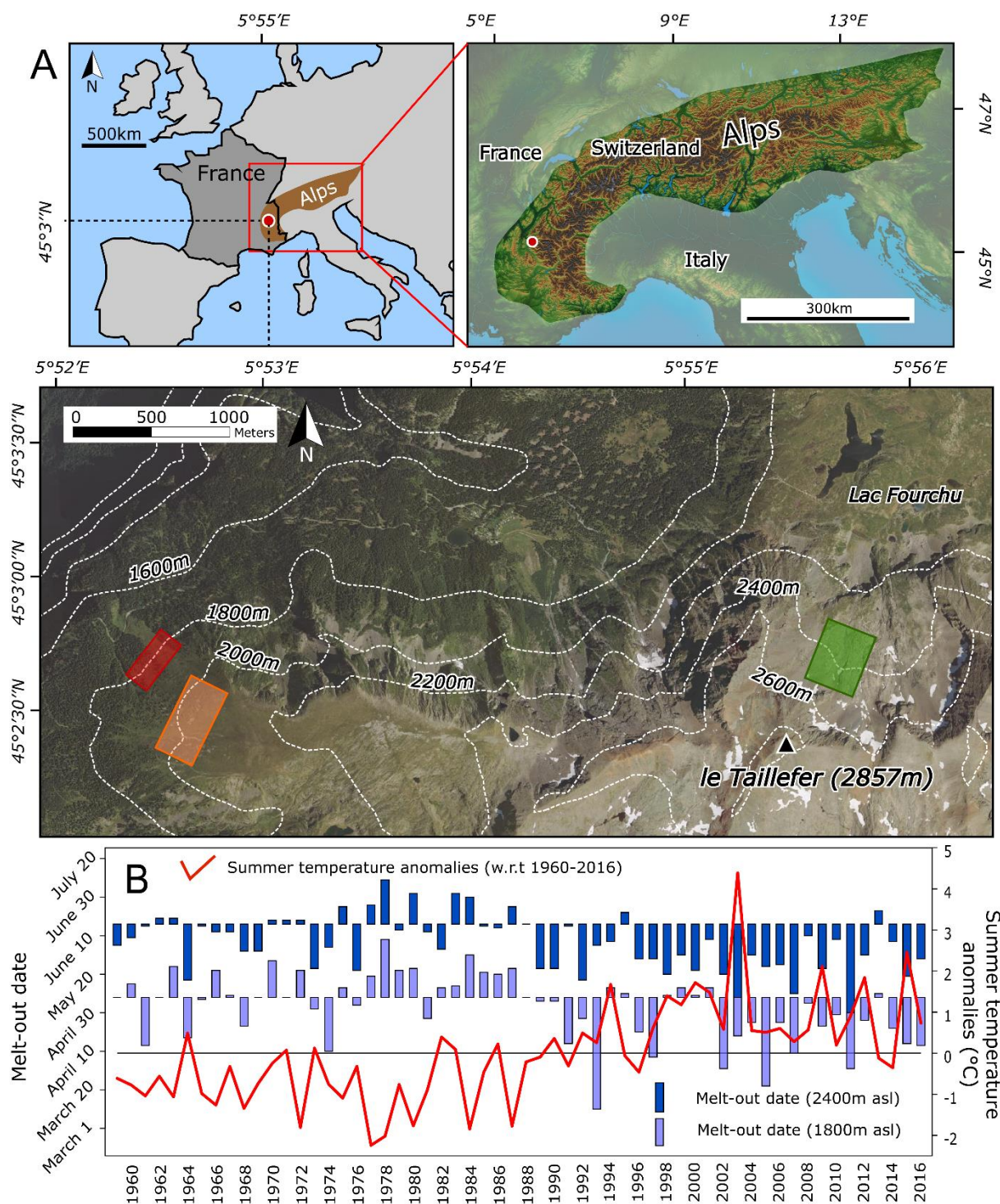
139 *Rhododendron ferrugineum* L. is the dominant mountain shrub of the subalpine belt in the
140 siliceous Alps (Ozenda, 1985). It is distributed from about 1600 to 2500 m asl, where it can
141 form large heathlands or grow in localized patches (Escaravage et al., 1997). The high local
142 abundance of the species can be attributed to complementary sexual and vegetative reproductive
143 strategies (Doche et al., 2005) which enable *R. ferrugineum* to outcompete other plants (Pornon
144 and Doche, 1996) and to reach a 90–100% cover after 150–250 years (Pornon and Doche,
145 1995). *R. ferrugineum* provides an ideal model to study the long-term effects of climate on
146 radial growth due to its high longevity, estimated to be up to three centuries (Escaravage et al.,
147 1998), as well as its clearly identifiable annual rings discriminated by a band of radially aligned,
148 thick walled latewood fibers, flattened along the ring boundary (Francon et al., 2017).

149 *Study area*

150 The study area is situated in the northern French Alps (Fig. 1), on a northwest-facing slope in
151 the Taillefer massif. At Taillefer, *R. ferrugineum* is the dominant species (80–100% cover) of
152 above-treeline dwarf shrub heathlands. The species developed on abandoned pastures between
153 1900 and 2100 m asl and is intermixed with *Sorbus* sp. and *Vaccinium* sp. along with scattered
154 *Picea abies* and *Pinus uncinata* trees. Beyond this altitude, heathlands become more fragmented
155 and are mixed with patches of alpine meadows and scree. Isolated patches of *R. ferrugineum*
156 are observed up to ~2500 m asl. Shrub individuals were sampled along an elevational gradient,

157 at three sites located at (i) 1800-1850 m (SAL1800), (ii) 1950-2050 m (SAL2000) and (iii)
158 2300-2500 m asl (CN2400). SAL1800 and SAL2000 are located at the Côte des Salières (SAL,
159 45°02'N, 5°52'E, Fig. 1) on a northwest-facing slope with slope angles ranging from 23° to 33°.
160 CN2400 is located in the Combe Nord (3 km east of SAL, 45°02'N, 5°55'E, Fig. 1) on a north-
161 facing slope (25°). At SAL1800 and SAL2000, bedrock consists of amphibolite and gneissic
162 gabbro (Doche et al., 2005). SAL1800 and SAL2000 heathlands have developed on stony,
163 ochre-brown humic acidic soils (Pornon et al., 1997). At CN2400, *R. ferrugineum* individuals
164 grow on shallow and discontinuous soils developed on talus slopes and weathered rock
165 outcrops.

166 Climate of the Taillefer massif reflects a transition between the wet oceanic Pre-Alps
167 (Chartreuse, Vercors) and the intra-alpine Oisans massif, with the latter being characterized by
168 a more continental climate with drier summers (Pautou et al., 1992). Daily reanalysis from the
169 SAFRAN meteorological system (Durand et al., 2009a) was used to characterize climatic
170 conditions along the elevational gradient (Fig. 1B). Over the period 1959-2016, mean annual
171 air temperatures were 4.2°C, 3.3°C, and 1.4°C at SAL1800, SAL2000 and CN2400,
172 respectively. The melt-out date occurred on average on May 2 at 1800 m asl, and roughly one
173 month later at 2400 m asl (June 6).



174

175 Figure 1: (A) Location of the study sites, Côte des Salières (SAL1800, red; SAL2000, orange) and
 176 Combe Nord (CN2400, green) in the Taillefer massif (French Alps). (B) Summer (May-August)
 177 temperature anomalies (1959-2016) as well as melt-out dates at 1800 (light blue) and 2400 m asl (dark
 178 blue) for the 1959-2017 period. Meteorological data were extracted from the SAFRAN-Crocus re-
 179 analysis datasets (Durand et al., 2009a, 2009b).

180

181 *Sample collection and preparation*

182 A total of 80 randomly selected *R. ferrugineum* individuals were sampled at the three sites: 36
183 at SAL2000 in October 2015, 17 at SAL1800, and 27 at CN2400 in October 2016. Individuals
184 were sampled at a minimum distance of four meters from each other to avoid the sampling of
185 the same clone (Escaravage et al., 1998). Locations were recorded with metric precision using
186 a Trimble GeoExplorer GNSS (Global Navigation Satellite System) unit. Three to six wood
187 sections were cut per individual on the main stems, starting at the root collar and then every 10-
188 20 cm to the stem extremity. This approach was used in order to apply the serial-sectioning
189 method, consisting of repeated growth-ring width measurements and cross dating at the intra-
190 stem level (Kolishchuk, 1990).

191 To ensure precise detection of all rings, 20 μm thick cross sections were prepared from each
192 sample using a slide microtome. Cross sections were then stained using Safranin and Astra
193 Blue, and permanently fixed on microslides with Canada balsam (Schweingruber et al., 2011).
194 High-resolution digital pictures were taken using a Carl Zeiss Axio Observer Z1 coupled to a
195 Zeiss AxioCam MR R3 camera under 40–100 magnification. Individual images were merged
196 automatically to cover the whole cross-sections by using the Zen 2011 software.

197 *Crossdating and chronology development*

198 Width of individual growth rings were measured from digital images with CooRecorder 7.6
199 (CYBIS Elektronik & Data AB) along three radii of the cross-sections to detect wedging rings.
200 Radial measurements along the chosen radii were supplemented by careful visual inspection of
201 each cross section to eliminate annual growth underestimation caused by partially missing
202 rings. Cross-dating was based on a three-step procedure involving a comparison of growth
203 curves (i) between three radii measured within a single cross section, (ii) among the mean
204 growth curves of all sections within individual plants, and finally (iii) between the mean growth

205 curves of all shrubs of a given site. The output of visual crossdating was statistically checked
206 with COFECHA (Holmes, 1994).

207 After cross-dating, each individual mean series was standardized (Cook and Kairiukstis, 1990;
208 Fritts, 1976) with a double-detrending process in ARSTAN (Cook, 1987). We first selected a
209 negative exponential function to eliminate non-climatic trends (e.g. age-related growth trend
210 and other potential biological effects) referred to as Neg-Exp chronologies. In addition, we
211 fitted a cubic smoothing spline, preserving 50% of the variance at a wave-length of 32 years so
212 as to remove the effect of localized disturbance events (Cook and Peters, 1981) hereafter
213 referred to as detrended chronologies. In both approaches, outputs referred as growth indices
214 were averaged by year using a bi-weighted robust mean aimed at reducing the influence of
215 outliers and at developing mean standardized site chronologies (Cook and Peters, 1981). The
216 resulting growth indices are referred to as ring-width indices (RWI).

217 Several descriptive statistics were then applied to detrended chronologies using the *dplR*
218 package, including standard deviation (SD), first-order autocorrelation (AC), mean sensitivity
219 (MS), mean inter-series correlation (Rbar), and expressed population signal (EPS; Bunn, 2008)
220 in R 3.3.2 (R Core Team, 2016). Running Rbar and EPS were computed at each site using a 30-
221 year moving window with a 29-year overlap to illustrate changes in the strength of common
222 patterns of radial growth over time. We used the commonly applied quality threshold of $EPS \geq$
223 0.85 to determine the reliability of our chronologies. As shrubs may potentially retain climate-
224 driven, low frequency variations in the raw data (decadal growth variations), Neg-Exp
225 chronologies were used to detect potential impacts of decadal-scale climatic fluctuations on
226 radial growth. Indices from the double-detrending procedure were used for climate-growth
227 correlations and climate-growth modeling in relation to high-frequency (interannual) growth
228 variations.

229 *Meteorological series*

230 At each plot, daily meteorological and snow time series were obtained from the SAFRAN-
231 Crocus coupled snowpack-atmosphere model. The SAFRAN reanalysis combines *in-situ*
232 meteorological observations with synoptic-scale meteorological fields to provide continuous
233 time series of meteorological variables at hourly resolution and for elevation bands of 300 m
234 within areas, referred to as “massifs” (Oisans in the case of this study), assumed to be
235 horizontally homogenous (Durand et al., 2009a). The dataset extends back to 1958. SAFRAN
236 meteorological fields are used to drive a land surface model, the ISBA-Crocus soil and
237 snowpack model. This tool provides corresponding reanalysis of snow conditions and
238 underlying ground temperature for the same time span as SAFRAN reanalysis (Durand et al.,
239 2009b; Vionnet et al., 2012). To quantify ground temperature, we extracted values for the
240 uppermost soil layer with a thickness of 1 cm.

241 SAFRAN meteorological fields corresponding to the sampling sites were extracted according
242 to their elevation, aspect, and slope angles (Lafaysse et al., 2013). Meteorological data were
243 interpolated from the neighboring 300-m elevation bands, and incoming shortwave radiation
244 data was adjusted by using the prevailing aspect and slope angle. The ISBA-Crocus models
245 runs were performed specifically for the sites. Vegetation was represented in a simplified
246 manner in the simulations, assuming grassy conditions so as to simulate typical snow conditions
247 and underlying ground temperature for open areas, therefore neglecting small-scale interactions
248 between vegetation, topography, and snowpack. We then extracted hourly air temperature and
249 precipitation sums as well as daily snow depth and uppermost ground layer temperatures (6:00
250 UTC) for the period 1959-2017. The data were carefully visually checked to detect extreme
251 temperature events that could be linked with marked growth reduction. Monthly minimum,
252 mean, and maximum air temperature, monthly precipitation sums, snow depth, and duration,
253 melt-out date, sum of snow-free growing degree days (SFGDD) and daily uppermost ground

254 layer temperature series were computed from the same datasets. The snow melt-out date was
255 defined as the last day when snow cover reached the mean height of the shrub canopy at *c.* 50
256 cm for SAL1800 and SAL2000, and at *c.* 30 cm for CN2400. SFGDD were calculated for
257 periods with snow-free ground and daily air mean temperatures above zero degrees. SFGDD
258 series were calculated from melt-out date to August 31.

259 Given that previous work identified a shift toward earlier snow melt-out in the study region
260 occurring during the late 1980s (Dedieu et al., 2016); we applied a breakpoint analysis to the
261 time-series of melt-out dates. This preliminary analysis points to a significant tipping point in
262 1988, which is consistent with regional-scale studies (Reid et al., 2016). At 2400 m asl, the
263 melt-out date thus advanced on average from June 14 (1959-1988) to May 28 (1989-2016). At
264 the same time, mean May temperatures increased from 1.7°C to 3.5°C. At 1800/2000m, a shift
265 of 19 days is observed for the melt-out date and an increase of 25% in SFGDD is observed. As
266 a consequence, climate-growth analyses were systematically performed separately for the
267 subperiods 1959-1988 and 1989-2016.

268 *Statistical analysis of climate-growth relationships*

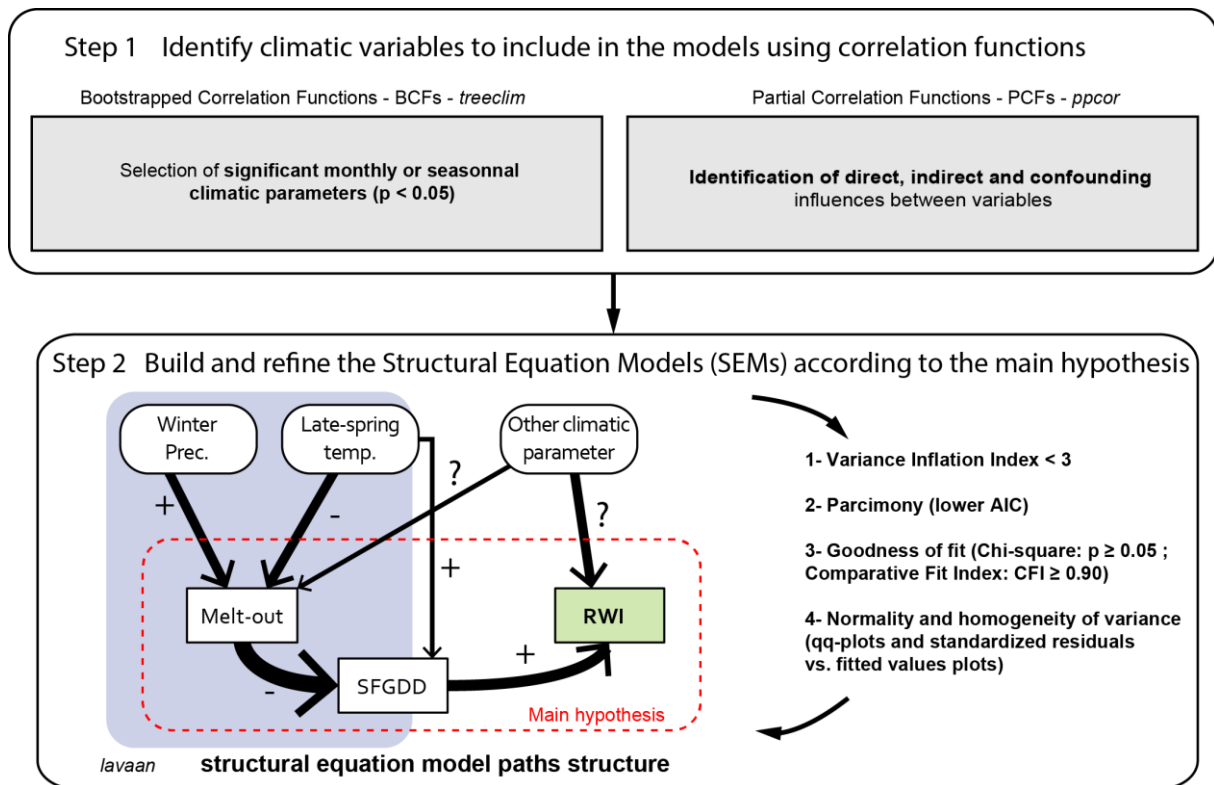
269 Structural Equation Models (SEMs, Grace, 2006; Kline, 2011) enable (i) decomposition of total
270 effects into direct and indirect types, and (ii) comparison of alternative models using indices of
271 goodness of fit (Kline, 2011; Mitchell, 1992). SEMs have been used in previous ecological
272 studies to investigate e.g. the impacts of shrub expansion on species richness and plant diversity
273 (Boscutti et al., 2018), the relation between climate and mountain plant productivity (Choler,
274 2015; Jonas et al., 2008; Madrigal-González et al., 2017, 2018) or the relation between tree-
275 ring width and sea surface temperature in Mexican dry forests (Brienen et al., 2010). Although
276 SEMs have been used quite rarely in dendroecology to date, they can indeed improve our
277 understanding of the concurrent effects that snow cover climatic variables have on growth. The
278 following two-step procedure was used to build models for each site: (Fig. 2):

279 (i) bootstrapped correlation functions (BCFs) between the detrended chronologies, mean
280 monthly air temperature (°C), monthly precipitation sums (mm), melt-out dates, and SFGDD
281 series were computed with the *Treeclim* package (Zang and Biondi, 2015) in R (R Core Team,
282 2016) to identify climate variables that are significantly correlated ($P < 0.05$) with radial growth.
283 To identify direct and indirect drivers of radial growth, we also computed partial correlation
284 functions (PCFs); and

285 (ii) SEMs were developed with the “*Lavaan*” package (Rosseel, 2012) in R. The structure of
286 the hypothetical SEM path structure (see Fig. 2) requires the incorporation of available *a priori*
287 knowledge (Pérez-de-Lis et al., 2016). In this study, direct effects are given as standardized
288 path or partial regression coefficients. According to the hypothesis formulated in the
289 introduction, we considered SFGDD as a direct driver of radial growth, while melt-out timing
290 was incorporated as an indirect parameter through its mediating effect on growing season
291 length. The latter parameters formed the backbone of the SEMs at each site, while additional
292 climatic variables significantly correlated ($p < 0.05$) with radial growth (steps 1-2) were added
293 as explanatory variables. To derive comparable estimates, we standardized all quantitative
294 predictors to a mean of zero and to a standard deviation of one. To prevent any effect of
295 multicollinearity among explanatory variables, we used variance inflation factors (VIF).
296 Collinearity was assessed with a cut-off value of 3 (Zuur et al., 2010). To compare the
297 competing models, each model was first evaluated with the Akaike Information Criterion (AIC,
298 Akaike, 1981) for which lower values correspond to more parsimonious models. We thereafter
299 employed the Chi-square (χ^2) difference statistic to control the overall fit and to verify whether
300 the model was consistent with the data covariance matrix (p cut-off ≥ 0.05) (Kline, 2011). In
301 addition, we computed the CFI (Comparative Fit Index, Bentler, 1990) with a CFI cut-off \geq
302 0.90. Assumptions of normality and homogeneity of variance were controlled for every

303 endogenous variable in the SEMs using qq-plots and standardized residuals vs. fitted values
 304 plots (see Fig. S1 in supplementary material).

305



306

307

308 Figure 2: Diagram of the 2-step procedure adopted for the development of the Structural Equation
 309 Models (SEMs). First (step 1), Bootstrapped Correlation Functions (BCFs) are used to identify climatic
 310 variables that potentially have a direct or indirect effect on Ring-Width Indices (RWI) at the monthly or
 311 seasonal scales. Relationships with SFGDD and Melt-out dates were also tested. Climatic variables were
 312 then tested using Partial Correlation Functions (PCFs) for direct, indirect or confounding effects on
 313 RWI. Second (step 2), SEMs are built according to the main hypothesis (Melt-out timing → SFGDD →
 314 RWI) and with other climatic parameters selected in step 1. Collinearity, parsimony, goodness of fit and
 315 main assumptions (normality and homogeneity of variance) were controlled and the SEM structure was
 316 potentially refined.

317 Results

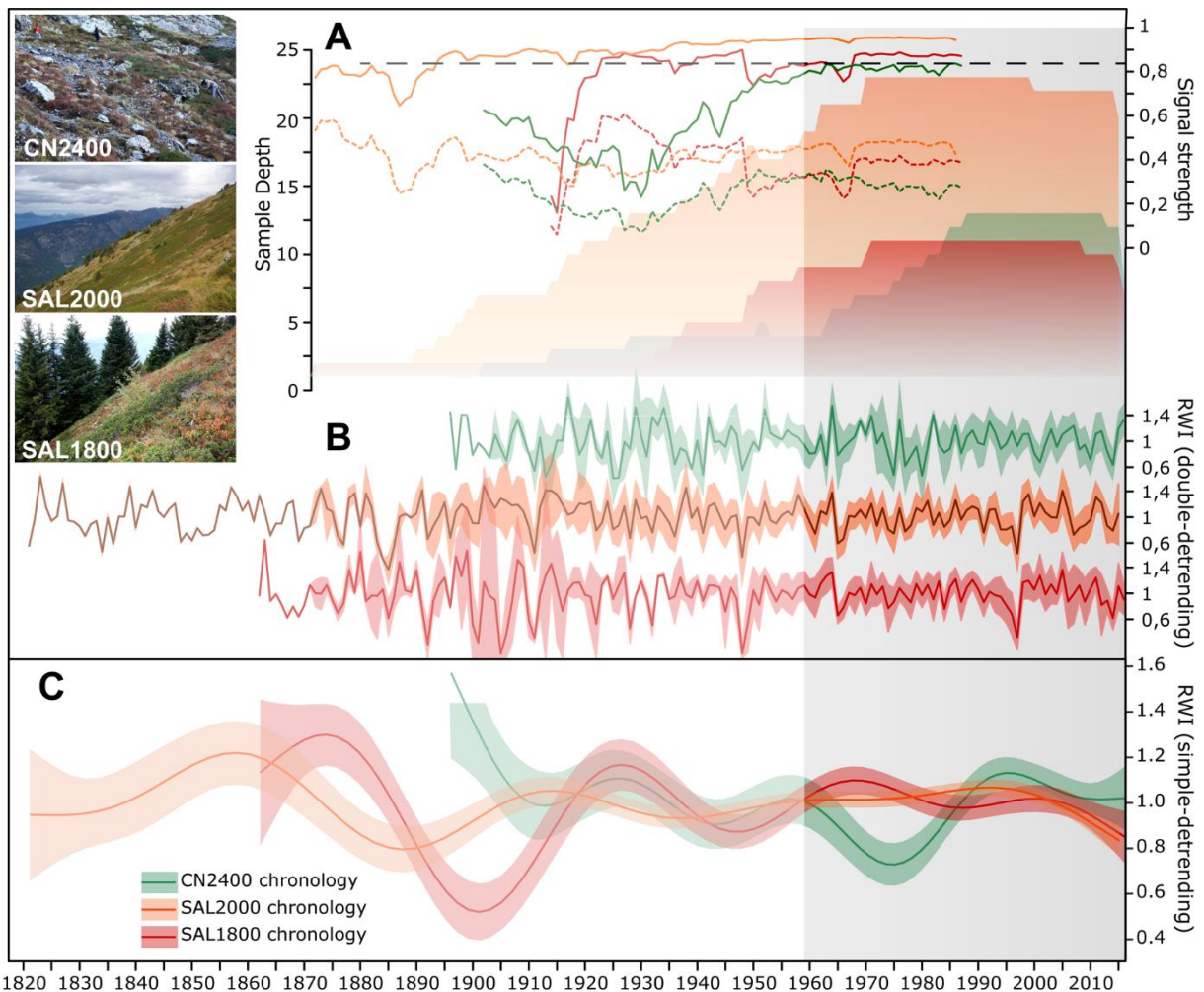
318 Chronology statistics

319 A total of 11, 24, and 14 *R. ferrugineum* individuals were included in the SAL1800 (1826-
 320 2016), SAL2000 (1821-2015) and CN2400 (1896-2016) chronologies, respectively (Fig. 3 A,
 321 B) corresponding to rejection rates (e.g. the percentage of misdated individuals) of 35, 33, and
 322 48% of the samples. Cross-correlations between standardized chronologies over the period

323 1960-2016 yielded r values of 0.80 (SAL1800-SAL2000), 0.46 (SAL2000-CN2400) and 0.30
324 (SAL1800-CN2400). Wood productivity – estimated as the mean annual growth between
325 cambial age 20 and 39 – was 0.17 mm at SAL1800, 0.16 mm at SAL2000, and thus significantly
326 larger than the values obtained at CN2400 (0.12 mm, ANOVA $p < 0.001$). Descriptive statistics
327 computed for the detrended chronologies (Fig. 3B) are given in Table 1. Mean sensitivity values
328 were comparable at SAL1800 (0.34) and CN2400 (0.31), but lower at SAL2000 (0.26). The
329 highest inter-series correlations ($R_{bar} = 0.41$), EPS (0.94) and AC values (0.22) were observed
330 at SAL2000. At SAL1800 and CN2400, lower R_{bar} and EPS values (slightly below the 0.85
331 threshold at CN2400) were found for the period covered by meteorological series (1959-2016),
332 thereby pointing to higher inter-individual ring-width variability.

333 Table 1: Characteristics of *R. ferrugineum* raw ring-width chronologies: length, mean age, median ring-
334 width. Statistics computed for detrended chronologies: standard deviation (Std. dev.), signal strength
335 (R_{bar} and EPS, computed only from 1959 onwards), mean sensitivity (MS) and first order
336 autocorrelation (AC).

Chronology	Raw ring-width chronologies				Detrended ring-width chronologies				
	First year	Last Year	Mean age	Median ring-width	Std. dev.	Mean R_{bar} (1959-2016)	Mean EPS (1959-2016)	MS	AC
SAL1800	1862	2016	81	0.171	0.281	0.321	0.86	0.338	0.136
SAL2000	1821	2015	86	0.159	0.246	0.412	0.94	0.257	0.221
CN2400	1896	2016	56	0.117	0.265	0.278	0.82	0.314	0.008



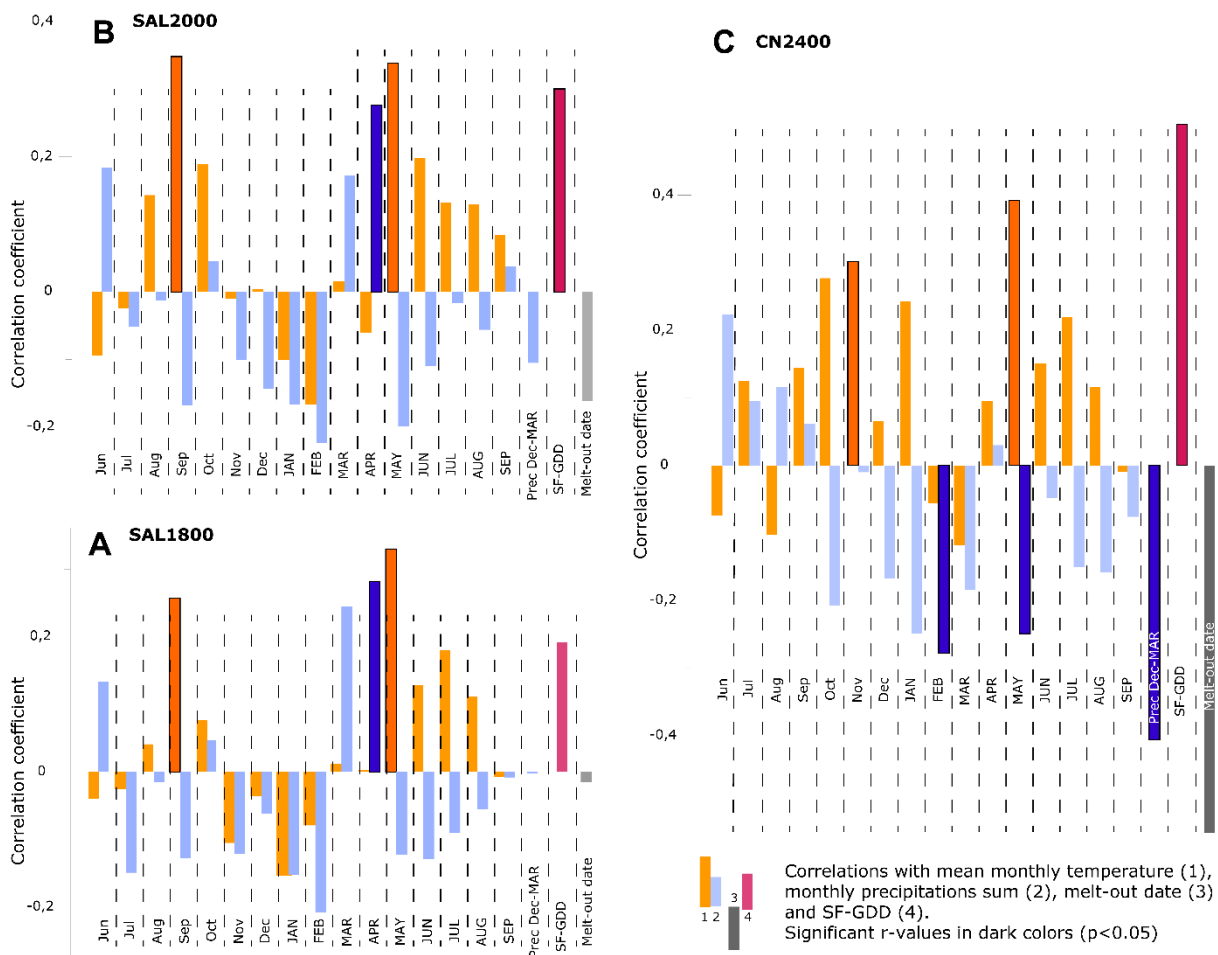
337
 338 Figure 3: (A) Sample depth (colored areas) and running detrended chronologies signal strength:
 339 Expressed Population Signal (EPS, solid lines) and common variance between single growth-ring series
 340 in a chronology (Rbar, dotted lines) were computed using a 30-year moving window. Colored areas
 341 indicate sample depth. The EPS threshold (0.85) is shown by the black dotted line. (B) Standard growth-
 342 ring chronologies of *R. ferrugineum* with ribbons designating Ring-Width Indices (RWI) \pm 1 SD. (C)
 343 Neg-Exp chronologies smoothed with a GAM-smoothing, ribbons indicate the 95% confidence
 344 intervals. The grey area corresponds to the period analyzed.

345 *Bootstrapped correlation functions (BCFs) and partial correlation functions (PCFs)*

346 Results from the bivariate bootstrapped correlation function analyses are summarized in Fig. 4.

347 May temperatures (year N; $r = 0.33, 0.34, 0.40$ at 1800, 2000, and 2400 m asl, respectively, all
 348 with $p < 0.05$) were the only statistically significant climatic driver of radial growth observed in
 349 all *R. ferrugineum* chronologies. More generally, positive correlations (albeit not significant)
 350 were observed between summer temperature of year N (June, July, and August) and radial
 351 growth at each site. Similar BCF profiles were observed at SAL1800 and SAL2000,

352 characterized by positive significant correlations with September (year N-1) temperatures ($r =$
 353 0.26 and $r = 0.35$, $p < 0.05$) and April precipitation sums ($r = 0.28$, $r = 0.28$, $p < 0.05$). By contrast,
 354 at CN2400, the response to fall (N-1) temperature was delayed to October ($r = -0.28$, $p = 0.06$)
 355 and November ($r = -0.30$, $p < 0.05$). The response of *R. ferrugineum* to snow melt-out date and
 356 SFGDD was particularly acute at 2400 m asl. The correlation between ring-width indices and
 357 SFGDD increased from low to high elevation sites, with $r = 0.18$ ($p = 0.18$) at SAL1800, $r = 0.28$
 358 ($p < 0.05$) at SAL2000, and $r = 0.51$ at CN2400 ($p < 0.001$). Radial growth also appeared to be
 359 more limited by melt-out date at CN2400 ($r = -0.56$, $p < 0.001$) and winter precipitation ($r = -$
 360 0.41 , $p < 0.01$) as compared to $r = 0$ at SAL1800 (Fig. 4).



361

362 Figure 4: Monthly bootstrapped correlation functions (BCFs) analysis between *R. ferrugineum* radial
 363 growth chronologies at SAL1800 (A); SAL2000 (B); and CN2400 (C), monthly mean temperatures,
 364 monthly precipitation sums, previous December to current March precipitation sums (Prec dec-MAR),
 365 SFGDD and snow melt-out date for the period 1959–2016. Months of the year preceding ring formation

366 (N-1) are given with lowercase letters, and months of the year (N) of ring formation are shown with
 367 capital letters.

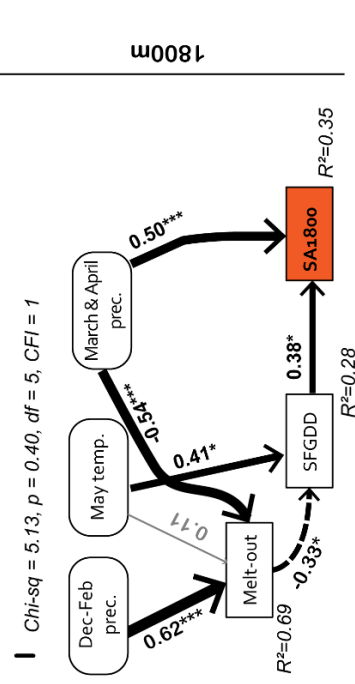
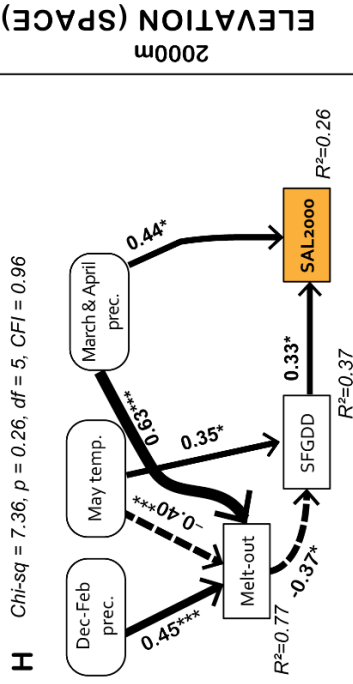
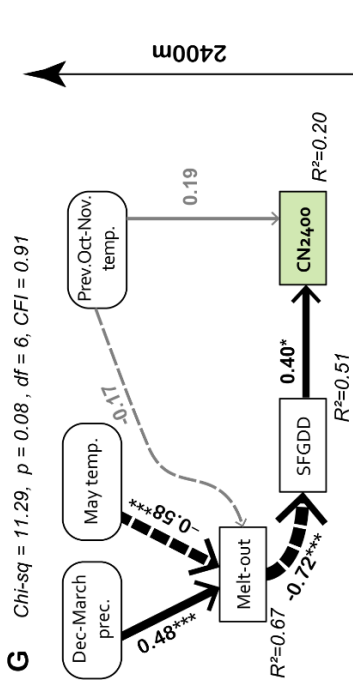
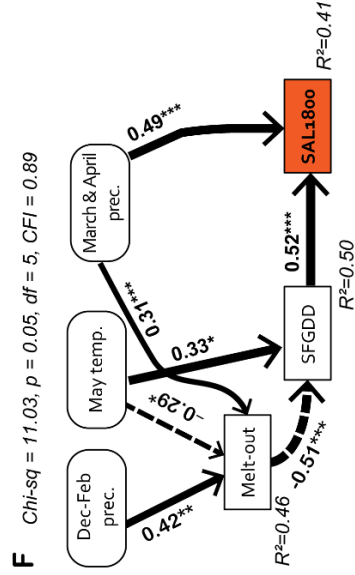
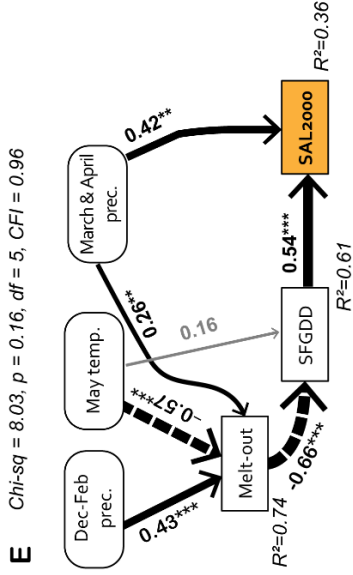
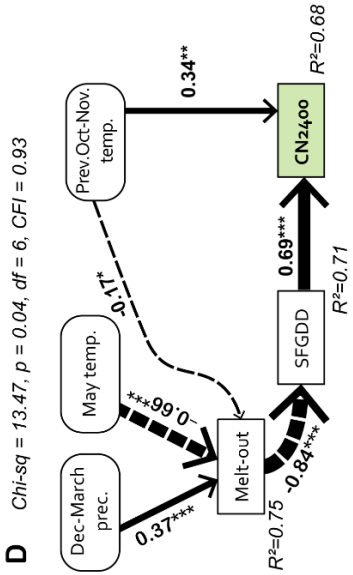
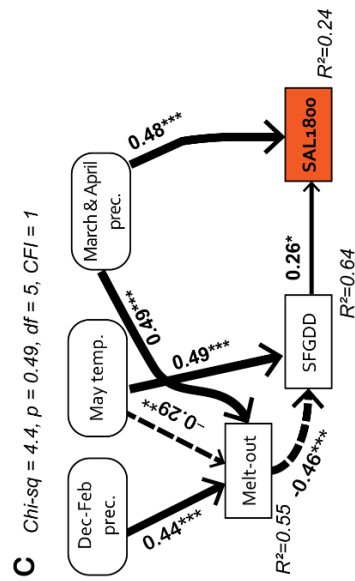
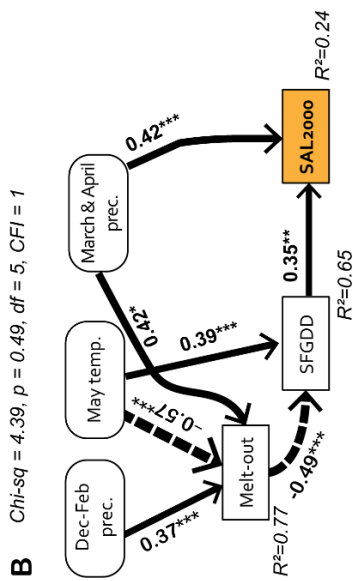
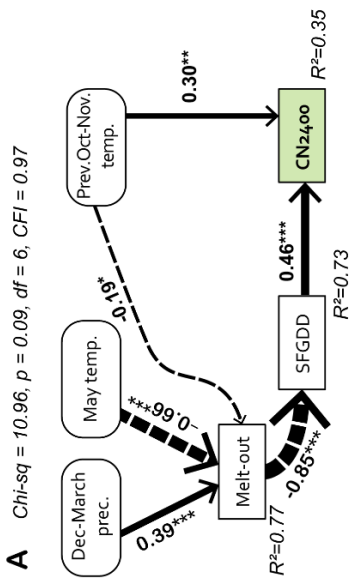
368 At our study sites, melt-out timing, late winter precipitation and May temperature are correlated,
 369 therefore partial correlations between tree-ring growth and the latter variables were performed.
 370 At CN2400, PCFs computed between radial growth, May temperature and precipitation or
 371 winter precipitation were not significant when melt-out timing was included as a control
 372 variable (Table 2). In other words, this indicates that the latter climatic variables have no impact
 373 on radial growth when melt-out-timing is held constant. Conversely, at SAL1800 and
 374 SAL2000, correlations between shrub chronologies, May temperature and March/April
 375 precipitation totals remain highly significant in the absence of melt-out timing fluctuations
 376 (Tab. 2). One can thus conclude that the correlations between our shrub ring width chronology
 377 and May temperature and late winter precipitation totals are 0.33 and 0.47 ($p < 0.05$),
 378 respectively at SAL1800 if adjusted for the effects of melt-out timing. At SAL2000, the partial
 379 coefficients reveal the critical influence of May temperature ($r = 0.32$, $p < 0.05$) and Mar-Apr
 380 precipitation ($r = 0.48$, $p < 0.001$) on radial growth.

381 Table 2: Partial Correlations Functions (PCFs) and their significance computed between climatic
 382 parameters and ring width indices (RWI) at SAL1800, SAL2000 and CN24000 controlling for melt-out
 383 timing. Significant relationships ($p < 0.05$) are given in bold. “na” means that the partial correlation was
 384 not computed, as no effect on radial growth was detected in the Bootstrapped Correlation Functions for
 385 the corresponding climatic variable.

Effect	SAL1800		SAL2000		CN2400	
	Corr.	Signif.	Corr.	Signif.	Corr.	Signif.
May temperature	0.33	0.01	0.32	0.02	0.03	0.84
March + April precipitation	0.47	0.00	0.48	0.00	na	na
Winter precipitation	na	na	na	na	-0.10	0.45
May precipitation	na	na	na	na	-0.08	0.56

386

387 *Structural equation modeling*



1960-1988 1989-2016

TIME

1960-2016

FULL PERIOD

ELEVATION (SPACE)

2400m

2000m

1800m

389 Figure 5: Results of structural equation models (SEMs) exploring the effects of spring snow-cover
390 duration (Melt-out) on Snow-Free Growing Degree Days (SFGDD), and the effects of SFGDD and other
391 climatic parameters (March and April precipitation totals at SAL1800/2000, previous September
392 temperature at SAL2000 and previous October-November temperature at CN2400) on shrub ring width
393 indices (RWI) at different sites (A, D, G: 1800 m asl, SAL1800; B, E, H: 2000 m asl, SAL2000 and C,
394 F, I: 2400 m asl, CN2400). SEMs were performed for the period 1960-2016 (A, B, C) and two sub-
395 periods: 1960-1988 (D, E, F) and 1989-2016 (G, H, I). Winter precipitation totals and May temperature
396 effects on Melt-out timing as well as the direct effect of May temperature on SFGDD are also
397 represented. Colored boxes represent measured RWI, white boxes represent intermediate climate
398 parameters and rounded white boxes represent monthly or seasonal meteorological data. Black solid (or
399 dotted) arrows indicate unidirectional positive (negative) significant relationships (at $p < 0.05$) among
400 variables. Grey arrows indicate non-significant relationship ($p > 0.05$). The thickness of the paths was
401 scaled to the magnitude of the standardized regression coefficient (shown besides the arrows). Multiple
402 R^2 are given next to the box of the respective response variable. Significance levels are denoted by ***
403 ($p < 0.001$), ** ($p < 0.01$), * ($p < 0.05$). Chi-square and CFI values indicate goodness of fit.

404

405 Results from BCFs and PCFs were used to determine the direction and strength of correlations
406 between climate variables and the shrub ring chronologies implemented in the path diagrams
407 of each structural equation model over the period 1960-2016 (Figs. 5A-C). At each site, as
408 stated in our initial hypotheses (Fig. 2), path diagrams were designed to disentangle the
409 respective impacts of SFGDD, melt-out timing, winter precipitation and spring temperatures on
410 shrub radial growth. In addition to the latter variables, fall temperatures (N-1, CN2400,
411 SAL2000) and spring precipitation (SAL1800, SAL2000), significantly correlated to shrub ring
412 records (BCFs), were added as direct predictor variables. SEMs computed for the periods 1960-
413 2016 displayed Chi-square p-values above 0.05 and CFI higher than the 0.9 cut-off. At the three
414 sites, the proportion of the variance in the dendrochronological series that could be explained
415 by the climatic variables increased with elevation ($R^2 = 0.35, 0.24, 0.24$ at CN2400, SAL2000
416 and SAL1800, respectively). However, the effect of SFGDD on shrub ring records increased
417 from 0.26 standard deviation units as a result of change of one standard deviation in SFGDD at
418 1800 m ($p < 0.05$) to 0.35 ($p < 0.01$) at 2000 m and to 0.46 ($p < 0.001$) at 2400 m asl. Significant
419 relations between climatic variables and radial growth differed along the elevational gradient.
420 At CN2400, SFGDD variability is the main driver of radial growth, which is significantly
421 related to melt-out-timing (path coefficient of -0.85, $p < 0.001$). Melt-out was in turn directly

422 conditioned by May temperature (-0.66, $p < 0.001$), winter precipitation (0.39, $p < 0.001$) and –
423 to a lesser extent – by previous late-autumn temperature (-0.19, $p < 0.05$).

424 At SAL2000, SFGDD, spring precipitation and previous fall temperature show comparable,
425 statistically significant impacts on shrub radial growth. Interannual variability of SFGDD
426 remains dependent on melt-out timing but is also directly driven by May temperature (Fig. 5B).
427 Finally, at 1800 m asl, the SEM differs from those obtained for the higher elevation sites. Albeit
428 significantly related to radial growth at SAL1800, SFGDD is not the main driver for shrub ring
429 width which appears to depend more strongly on March-April precipitation totals (0.48,
430 $p < 0.001$). At this elevation, SFGDD is driven by melt-out timing and May temperature (-0.46,
431 $p < 0.001$ and 0.49, $p < 0.001$, respectively).

432 *Stationarity of radial growth-climate relationships over time*

433 To evaluate the stationarity and consistency of radial growth-climate relationships, SEMs were
434 computed for the two sub-periods 1960-1988 and 1989-2016 (Fig. 5 D-I). The SEMs presented
435 good overall performances by passing the goodness of fit cutoffs of Chi-square $p > 0.05$ and CFI
436 > 0.90 except for the SEMs computed at CN2400 and SAL1800 for the period 1960-1988 ($\chi^2 =$
437 13.47, $p = 0.04$, CFI = 0.93 at CN2400 and $\chi^2 = 11.03$, $p = 0.05$, CFI = 0.89 at SAL1800).

438 Strikingly, we observe a loss of the explanatory powers of the SEMs for the recent period,
439 especially at CN2400 where the amount of variance in radial growth explained by climatic
440 variables decreased from 0.69 for the period 1960-1988 to 0.20 between 1989 and 2016. For
441 both subperiods, the dependence of radial growth on SFGDD thus decreased from 0.69
442 ($p < 0.001$) to 0.40 ($p < 0.05$), from 0.54 ($p < 0.001$) to 0.33 ($p < 0.05$), and from 0.52 ($p < 0.001$) to
443 0.38 ($p < 0.05$) at 2400, 2000, and 1800 m asl, respectively. In addition, the models illustrate
444 nicely that the dependence of SFGDD on melt-out dates and May temperatures remain highly
445 significant ($p < 0.001$) at CN2400, whereas their influence strongly decreased at SAL2000 and

446 SAL1800 after 1988. Similarities exist between the SEM computed at SAL2000 for the period
447 1960-1988 and at CN2400 for the period 1989-2016 (Fig. 5 E, G), especially with respect to
448 the correlations between May temperatures, melt-out timing, SFGDD and radial growth.
449 Similarly, comparable impacts of winter precipitations and May temperatures on melt-out dates
450 were observed in Fig. 5F and 5H. This evolution suggests a 200-400 m shift of the climatic
451 conditions and, to a lesser extent, of radial growth response to climate over the last 30 years.

452

453 **Discussion**

454 In this paper, we disentangled the impact of recent climate change, especially of earlier snow
455 melt-out, on radial growth in the widespread mountain shrub species *Rhododendron*
456 *ferrugineum* by sampling a total of 80 stems along an elevation gradient. The three multi-
457 decadal growth-ring chronologies developed from individuals sampled at 1800, 2000, and 2400
458 m asl (referred to as SAL1800, SAL2000, and CN2400) provide a unique perspective on
459 mountain shrub responses to climate variability in the context of recent climate changes (Myers-
460 Smith et al., 2015). We used Structural Equation Models (SEMs), rarely used in
461 dendroecological studies so far, to disentangle direct and indirect drivers of radial growth. Our
462 results clearly demonstrate an elevation-dependent response of *R. ferrugineum* to snow cover
463 duration and provide evidence for a divergence of radial growth responses to climate during
464 recent decades, given that climate-growth correlations have weakened since 1988. This study
465 also benefits from the hourly-resolution of meteorological as well as snow series from the
466 SAFRAN-Crocus dataset. The latter data, available at the elevations of the three study plots for
467 the period 1960-2017, are of a precision that is only rarely equaled in any previously published
468 alpine or arctic dendroecological study.

469 *Radial growth responses along the snow melt-out timing gradient*

470 At CN2400, results support the initial hypothesis that the amount of growing degree days during
471 the snow-free period (SFGDD) would impact *R. ferrugineum* radial growth strongly whereas
472 melt-out dates would act only as an indirect limiting factor on radial growth by conditioning
473 the length of the growing season. Results from SEMs show that SFGDD – controlled by melt
474 out dates – explained about 46% of radial growth variability over the period 1960-2016 and
475 about 70% of the variability between 1960 and 1988. At this elevation, the growing season is
476 short (85 days on average prior to August 31) and SFGDD totals are low (823°C on average for
477 the period 1959-2016). Snowmelt frequently occurs between early and mid-June and coincides
478 with peak annual temperatures and photoperiod, i.e. when the carbon gain of a single bright day
479 is at its maximum. Consequently, any variation in melt-out dates, even by a few days, can affect
480 SFGDD totals strongly, and can thus also explain the strong correlation between both variables
481 ($r = -0.85$, $p < 0.001$).

482 *R. ferrugineum* is an evergreen shrub that has developed an opportunistic growth strategy, able
483 to photosynthesize within two hours after snow removal (Larcher and Siegwolf, 1985). We can
484 therefore reasonably assume that the species will also benefit from an earlier growing season,
485 consistent with the correlation between SFGDD and radial growth. Our results are in line with
486 numerous studies from Arctic and Alpine environments, which demonstrated that the
487 accumulation of temperature above a certain threshold is a key factor driving growth through
488 cell division and differentiation (Hoch, 2015; Körner, 2003; Wheeler et al., 2016; Wipf, 2010)
489 and phenological transitions (Kudo and Suzuki, 1999; Molau et al., 2005). Results are also
490 consistent with (i) dendrochronological studies that demonstrated the negative effect of
491 snowpack duration on radial growth at the upper shrub limit in the Alps (Carrer et al., 2019;
492 Francon et al., 2017; Pellizzari et al., 2014) and (ii) manipulation experiments (Stinson, 2005;
493 Wheeler et al., 2016) showing increased productivity in case of artificial snow removal at sites
494 where melt-out dates occurred after late-May (Wipf and Rixen, 2010). Results from the Alps

495 differ from the wealth of studies in the Arctic, where a positive effect of snowpack was
496 highlighted. We can explain this discrepancy by the fact that, in the Arctic, the positive winter
497 precipitation effect is mostly related to snowpack thermal insulation, which protects plants from
498 the harsh external conditions but also promotes higher winter soil surface temperatures with
499 greater decomposition and nutrient release (Chapin, 2005; Hallinger et al., 2010). Furthermore,
500 Alpine snowpack tends to be deeper and winter temperatures milder compared to the Arctic,
501 and accordingly soil temperatures less sensitive to a slight change in snow accumulation. In the
502 context of our study sites, root and vegetative shrub tissues are likely more protected from
503 persistent negative temperatures in the Alps than in the Arctic (Domine et al., 2016; Ernakovich
504 et al., 2014).

505 By contrast, at the lower sites (SAL1800, SAL2000), our results indicate that the weaker effects
506 of (i) snow cover duration on SFGDD and (ii) SFGDD on ring width can be explained by earlier
507 melt-out dates, occurring at these elevations between early and mid-May, when daily
508 temperatures (4.9°C and 6.4 °C in May on average for the 1960-2016 period at 2000 and 1800m
509 asl, respectively) and solar radiation have not yet attained peak values and are insufficient for
510 shrub growth. In addition, SFGDD at SAL1800 and SAL2000 (1316°C on average) are
511 significantly higher than those estimated at CN2400 and thus certainly less constraining for
512 plants to complete the phenological cycle and a complete carbon storage at the end of the
513 growing season. These hypotheses are consistent with experiments showing neutral to negative
514 impacts of early (i.e. late-April) artificial snow removal (Dorrepaal et al., 2006; Wipf et al.,
515 2006, 2009) at sites where natural early melt-out date would occur before mid-May. Wipf et al.
516 (2009) found a general decrease in shoot growth in mountain shrub species (*Empetrum nigrum*,
517 *Vaccinium myrtillus* and *V. uliginosum*) under earlier melt-out dates due to higher frost
518 exposure. In the specific case of *R. ferrugineum*, Malfasi and Cannone (2020) found that the
519 recruitment rate was favored by prolonged snow cover occurrence. In our case, the positive

520 effect of a longer growing season on radial growth can be similarly offset by the detrimental
521 impact of spring frost (Choler, 2015; Jonas et al., 2008) or drought (Wheeler et al., 2016).
522 Accordingly, we hypothesize that the positive correlations observed between low-elevation
523 chronologies and March-April precipitation sums could either reflect (i) the positive effect of
524 early spring precipitation on nutrient supply at the beginning of the growing season by
525 enhancing decomposition and nitrogen mineralization right after snow melt-out (Baptist et al.,
526 2010; Ernakovich et al., 2014) or (ii) the protective effect of late snowfalls against late frost
527 (Choler, 2015; Jonas et al., 2008), irradiation (Neuner et al., 1999) or limited drought stress
528 during the subsequent growing season (Buchner and Neuner, 2003; Daniels and Veblen, 2004).

529 In the case of the Taillefer massif, a detailed analysis of meteorological conditions and radial
530 growth in 1997 is relevant in order to illustrate the detrimental effects of late frost. According
531 to the SAFRAN-Crocus reanalysis, melt-out occurred on approximately April 14 at lower
532 elevations (SAL1800 and SAL2000,) and on May 31 at CN2400. At lower elevations, spring
533 1997 was the coldest since 1959 at the ground level. Immediately after melt-out, two cold
534 episodes with two extreme freezing periods occurred between April 14 and 24 and between
535 May 6 and 9. Ground level temperatures reached their absolute minimum on April 17 at -7.3°C.
536 The same year, a majority of *R. ferrugineum* individuals from the two lower elevation sites
537 formed extremely narrow rings, whereas no significant growth reduction was observed at 2400
538 m asl where plants were still under snow. This suggests that very low productivity at SAL1800
539 and SAL2000 is linked to cellular damage associated with intense late frost which likely
540 damaged fine roots, leaves, buds, and the cambium (Inouye, 2000; Wipf et al., 2006; Wipf and
541 Rixen, 2010). However, the absence of other events comparable to 1997 in meteorological or
542 ring width series does not allow inference of robust relationships between late frost and radial
543 growth. Here, experimental testing using ecophysiological monitoring could be used to further
544 explore the effects of frost events on radial growth (Charrier et al., 2017).

545 *Climate warming, trend analysis and the divergence problem*

546 Our study demonstrates diverging effects of growing season length and snowmelt timing on
547 radial growth along the elevational gradient. At CN2400, the decadal growth trend follows that
548 of SFGDD, in line with findings from the Arctic (Myers-Smith et al., 2015a). In addition, at
549 lower elevation sites, our results also point to a divergence of radial growth as radial growth
550 did not track the SFGDD increase during more recent decades. These results concur with the
551 growth decline detected since the 1990s in shrub rings of *B. nana* and *S. glauca* from Western
552 Greenland, where reduced ring width was attributed to increasing moisture limitation (Gamm
553 et al., 2018). In the Taillefer massif, a weakening of the climatic signal is observed in shrub-
554 ring chronologies after 1988, a year that can be considered as a tipping point in the
555 meteorological series. Interestingly, comparable trends were reported for *B. nana* and *E.*
556 *hermaphroditum* in the central Norwegian Scandes, where the positive influence of summer
557 conditions was replaced by a negative response to May temperatures, over the last decades
558 (Weijers et al., 2018a, 2018b). These findings echo the “divergence problem” reported in trees
559 growing at circumpolar, northern latitudes (Briffa et al., 1998; D’Arrigo et al., 2008; Driscoll,
560 2005) and high-elevation sites (Büntgen et al., 2006, 2008). This body of evidence suggests
561 more complex and nonlinear growth responses of trees to a changing climate, thereby leading
562 to a decrease in year-to-year sensitivity of tree growth (i.e. “non-stationarity”) in previously
563 temperature-limited sites (D’Arrigo et al., 2008; Vaganov et al., 1999; Wilmking, 2005;
564 Wilmking et al., 2020). Potential causes for this divergence include warming-induced
565 thresholds of tree growth (D’Arrigo et al., 2004; Jochner et al., 2018), limitation of growth by
566 nutrient availability (Fajardo and Piper, 2017) or drought stress (Büntgen et al., 2006) or
567 interactions between these factors. In the case of low-stature alpine vegetation, frost damage
568 (Phoenix and Bjerke, 2016; Treharne et al., 2019) could also be assumed as a cause divergence,
569 and merits further investigation.

570 **Conclusion**

571 In this paper, we analyze annually resolved, statistically solid multi-decadal chronologies of 49
572 *R. ferrugineum* shrubs sampled along an elevational gradient in the French Alps. Results show
573 that a clear, elevation-dependent climatic signal exists in the growth-ring series covering the
574 period 1959-2016. Comparison of the SEMs along the elevational gradient shows that SFGDD
575 and, by extension, melt-out dates are the main drivers of radial growth at 2400 m asl. By
576 contrast, at lower elevations, melt-out dates have a limited effect on SFGDD, as the latter only
577 barely limit radial growth. In addition, meteorological and snowpack series from the model
578 SAFRAN-Crocus point to a breakpoint in 1988. In fact, since the late 1980s, melt-out dates
579 have advanced by an average of 17 to 19 days depending on elevation. Since 1988, our study
580 provides evidence of a recent divergence in radial growth, insofar as the increase in SFGDD
581 results in a weakening of the climatic signal in shrub ring-width chronologies, similar to the
582 divergence observed in trees at circumpolar and alpine sites. Moreover, at lower elevations
583 (1800 and 2000 m asl), an extremely narrow ring was formed in 1997 following a late frost
584 event. Albeit unique in the dendrochronological series, it illustrates the potential detrimental
585 effects of early melt-out dates on productivity. Accordingly, 1997 might well be an example of
586 extreme events that can be expected to become more frequent in a warmer climate. This non-
587 stationarity of climate-growth relationships suggests strong threshold effects in terms of
588 temperature and melt-out timing in a context of global warming.

589 This study shows that *R. ferrugineum* is particularly sensitive to local meteorological conditions
590 such as snow cover or frost events. For this reason and given its large occurrence above the
591 treeline in the Alps and Pyrenees (Francon et al., 2017; Gracia et al., 2007), we believe that this
592 species represents a valuable dendroecological indicator to document the response of alpine
593 vegetation to global warming over the last centuries. As such, *R. ferrugineum* could be used
594 easily to complement *Juniperus nana* in future dendroecological studies, even more so as both

595 species are characterized by a wide distribution above treeline and a life span of more than a
596 century (Carrer et al., 2019; Pellizzari et al., 2014, 2016). Yet, unlike *J. nana*, whose radial
597 growth is mainly driven by regional climate variability (Carrer et al., 2019), *R. ferrugineum*
598 seems to be very sensitive to fine-scale climatic variations induced by topography.

599 To further improve our understanding of the processes governing shrub growth in mountain
600 environments and to precisely define the values of the above-mentioned climatic thresholds,
601 including the potential impact of extreme climatic events, we recommend that future research
602 be directed in two directions. Firstly, more populations growing in contrasting topoclimatic
603 situations across the Alps should be sampled and compared with topoclimatic data. Secondly,
604 we plead for future work to combine field-based eco-physiological and microclimatic
605 monitoring (see e.g. Charrier et al. 2017), with remote sensing of landscape-scale vegetation
606 dynamics in alpine regions (see e.g. Carlson et al., 2017; Bayle et al. (2019).

607 **Acknowledgments**

608 This research was supported by the program ProXyCliM (2016–2017) funded by the CNRS
609 (Mission interdisciplinarité - RNMSH) and by the french national grant EC2CO-
610 Biohefect/Ecodyn//Dril/MicrobiEen, SNOWSHRUB. We wish to thank all who contributed to
611 the meteorological series data used in the analyses, especially Carlo Maria Carmagnola (Météo-
612 France - CNRS, CNRM, CEN). We are particularly grateful to Brigitte Girard (INRA, PIAF)
613 for her much appreciated help during the tedious phase of the laboratory. We acknowledge
614 Olivier Voldoire (GEOLAB, CNRS) for technical support. Rhododendron shrubs were sampled
615 with the help of Séverine Finet, and Robin Mainieri. We are also grateful to Frida Piper and
616 Jaime Madrigal González for insightful feedback on the manuscript. CNRM/CEN,
617 Irstea/ETNA and LECA are part of LabEX OSUG@2020.

618

619 **References**

- 620 Ackerman D, Griffin D, Hobbie SE, Finlay JC. 2017. Arctic shrub growth trajectories differ across soil moisture
621 levels. *Global Change Biology* **23** : 4294–4302. DOI: 10.1111/gcb.13677
- 622 Akaike H. 1981. Likelihood of a model and information criteria. *Journal of Econometrics* **16** : 3–14. DOI:
623 10.1016/0304-4076(81)90071-3
- 624 Anthelme F, Villaret J-C, Brun J-J. 2007. Shrub encroachment in the Alps gives rise to the convergence of sub-
625 alpine communities on a regional scale. *Journal of Vegetation Science* **18** : 355–362. DOI: 10.1111/j.1654-
626 1103.2007.tb02547.x
- 627 Baptist F, Yoccoz NG, Choler P. 2010. Direct and indirect control by snow cover over decomposition in alpine
628 tundra along a snowmelt gradient. *Plant and Soil* **328** : 397–410. DOI: 10.1007/s11104-009-0119-6
- 629 Bär A, Bräuning A, Löffler J. 2006. Dendroecology of dwarf shrubs in the high mountains of Norway – A
630 methodological approach. *Dendrochronologia* **24** : 17–27. DOI: 10.1016/j.dendro.2006.05.001
- 631 Bär A, Pape R, Bräuning A, Löffler J. 2008. Growth-ring variations of dwarf shrubs reflect regional climate signals
632 in alpine environments rather than topoclimatic differences. *Journal of Biogeography* **35** : 625–636. DOI:
633 10.1111/j.1365-2699.2007.01804.x
- 634 Bayle A, Carlson B, Thierion V, Isenmann M, Choler P. 2019. Improved Mapping of Mountain Shrublands Using
635 the Sentinel-2 Red-Edge Band. *Remote Sensing* **11** : 2807. DOI: 10.3390/rs11232807
- 636 Beniston M et al. 2018. The European mountain cryosphere: a review of its current state, trends, and future
637 challenges. *The Cryosphere* **12** : 759–794. DOI: 10.5194/tc-12-759-2018
- 638 Bentler P. 1990. Comparative fit indexes in structural models. *Psychological Bulletin* **107** : 228–246.
- 639 Bjorkman AD et al. 2018. Plant functional trait change across a warming tundra biome. *Nature* DOI:
640 10.1038/s41586-018-0563-7 [online] Available from: <http://www.nature.com/articles/s41586-018-0563-7>
641 (Accessed 2 October 2018)
- 642 Bjorkman AD et al. 2020. Status and trends in Arctic vegetation: Evidence from experimental warming and long-
643 term monitoring. *Ambio* **49** : 678–692. DOI: 10.1007/s13280-019-01161-6
- 644 Blok D, Sass-Klaassen U, Schaepman-Strub G, Heijmans MMPD, Sauren P, Berendse F. 2011. What are the main
645 climate drivers for shrub growth in Northeastern Siberian tundra? *Biogeosciences* **8** : 1169–1179. DOI:
646 10.5194/bg-8-1169-2011
- 647 Boscutti F, Casolo V, Beraldo P, Braidot E, Zancani M, Rixen C. 2018. Shrub growth and plant diversity along an
648 elevation gradient: Evidence of indirect effects of climate on alpine ecosystems. Carcaillet C (ed). *PLOS ONE* **13**
649 : e0196653. DOI: 10.1371/journal.pone.0196653
- 650 Brien RJW, Lebrija-Trejos E, Zuidema PA, Martínez-Ramos M. 2010. Climate-growth analysis for a Mexican
651 dry forest tree shows strong impact of sea surface temperatures and predicts future growth declines: CLIMATE-
652 GROWTH ANALYSIS OF A DRY FOREST TREE. *Global Change Biology* **16** : 2001–2012. DOI:
653 10.1111/j.1365-2486.2009.02059.x
- 654 Briffa KR, Schweingruber FH, Jones PD, Osborn TJ, Shiyatov SG, Vaganov EA. 1998. Reduced sensitivity of
655 recent tree-growth to temperature at high northern latitudes. *Nature* **391** : 678–682.
- 656 Buchner O, Neuner G. 2003. Variability of Heat Tolerance in Alpine Plant Species Measured at Different
657 Altitudes. *Arctic, Antarctic, and Alpine Research* **35** : 411–420. DOI: 10.1657/1523-
658 0430(2003)035[0411:VOHTIA]2.0.CO;2
- 659 Buchwal A, Rachlewicz G, Fonti P, Cherubini P, Gärtner H. 2013. Temperature modulates intra-plant growth of
660 *Salix polaris* from a high Arctic site (Svalbard). *Polar Biology* **36** : 1305–1318. DOI: 10.1007/s00300-013-1349-
661 x
- 662 Büntgen U, Frank D, Wilson R, Carrer M, Urbinati C, Esper J. 2008. Testing for tree-ring divergence in the
663 European Alps. *Global Change Biology* **14** : 2443–2453. DOI: 10.1111/j.1365-2486.2008.01640.x
- 664 Büntgen U, Frank DC, Nievergelt D, Esper J. 2006. Summer Temperature Variations in the European Alps, A.D.
665 755–2004. *Journal of Climate* **19** : 5606–5623. DOI: 10.1175/JCLI3917.1
- 666 Cannone N, Sgorbati S, Guglielmin M. 2007. Unexpected impacts of climate change on alpine vegetation.
667 *Frontiers in Ecology and the Environment* **5** : 360–364. DOI: 10.1890/1540-9295(2007)5[360:UIOCCO]2.0.CO;2

- 668 Carlson BZ, Corona MC, Dentant C, Bonet R, Thuiller W, Choler P. 2017. Observed long-term greening of alpine
669 vegetation—a case study in the French Alps. *Environmental Research Letters* **12** : 114006. DOI: 10.1088/1748-
670 9326/aa84bd
- 671 Carrer M, Pellizzari E, Prendin AL, Pividori M, Brunetti M. 2019. Winter precipitation - not summer temperature
672 - is still the main driver for Alpine shrub growth. *Science of The Total Environment* **682** : 171–179. DOI:
673 10.1016/j.scitotenv.2019.05.152
- 674 Chapin FS. 2005. Role of Land-Surface Changes in Arctic Summer Warming. *Science* **310** : 657–660. DOI:
675 10.1126/science.1117368
- 676 Charrier G, Nolf M, Leitinger G, Charra-Vaskou K, Losso A, Tappeiner U, Améglio T, Mayr S. 2017. Monitoring
677 of Freezing Dynamics in Trees: A Simple Phase Shift Causes Complexity. *Plant Physiology* **173** : 2196–2207.
678 DOI: 10.1104/pp.16.01815
- 679 Chen I-C, Hill JK, Ohlemuller R, Roy DB, Thomas CD. 2011. Rapid Range Shifts of Species Associated with
680 High Levels of Climate Warming. *Science* **333** : 1024–1026. DOI: 10.1126/science.1206432
- 681 Choler P. 2015. Growth response of temperate mountain grasslands to inter-annual variations in snow cover
682 duration. *Biogeosciences* **12** : 3885–3897. DOI: 10.5194/bg-12-3885-2015
- 683 Cook ER. 1987. The decomposition of tree-ring series for environmental studies. *Tree Ring Bulletin* **47** : 37–59.
- 684 Cook ER, Kairiukstis LA (eds). 1990. *Methods of Dendrochronology* . Springer Netherlands: Dordrecht
- 685 Cook ER, Peters K. 1981. The smoothing spline: a new approach to standardizing forest interior tree-ring width
686 series for dendroclimatic studies. *Tree Ring Bulletin* **41** : 45–53.
- 687 Daniels LD, Veblen T. 2004. Spatiotemporal Influences of Climate on Altitudinal Treeline in Northern Patagonia.
688 *Ecology* **85** : 1284–1296.
- 689 D'Arrigo R, Kaufmann RK, Davi N, Jacoby GC, Laskowski C, Myneni RB, Cherubini P. 2004. Thresholds for
690 warming-induced growth decline at elevational tree line in the Yukon Territory, Canada: THRESHOLDS FOR
691 WARMING-INDUCED GROWTH DECLINE. *Global Biogeochemical Cycles* **18** : n/a-n/a. DOI:
692 10.1029/2004GB002249
- 693 D'Arrigo R, Wilson R, Liepert B, Cherubini P. 2008. On the 'Divergence Problem' in Northern Forests: A review
694 of the tree-ring evidence and possible causes. *Global and Planetary Change* **60** : 289–305. DOI:
695 10.1016/j.gloplacha.2007.03.004
- 696 Dedieu J-P, Carlson B, Bigot S, Sirguey P, Vionnet V, Choler P. 2016. On the Importance of High-Resolution
697 Time Series of Optical Imagery for Quantifying the Effects of Snow Cover Duration on Alpine Plant Habitat.
698 *Remote Sensing* **8** : 481. DOI: 10.3390/rs8060481
- 699 Doche B, Franchini S, Pornon A, Lemperiere G. 2005. Changes of Humus Features along with a Successional
700 Gradient of *Rhododendron ferrugineum* (L.) Populations (Subalpine Level, Northwestern Alps, France). *Arctic,*
701 *Antarctic, and Alpine Research* **37** : 454–464. DOI: 10.1657/1523-0430(2005)037[0454:COHFAW]2.0.CO;2
- 702 Dolezal J et al. 2016. Vegetation dynamics at the upper elevational limit of vascular plants in Himalaya. *Scientific*
703 *Reports* **6** DOI: 10.1038/srep24881 [online] Available from: <http://www.nature.com/articles/srep24881> (Accessed
704 7 December 2018)
- 705 Domine F, Barrere M, Morin S. 2016. The growth of shrubs on high Arctic tundra at Bylot Island: impact on snow
706 physical properties and permafrost thermal regime. *Biogeosciences* **13** : 6471–6486. DOI: 10.5194/bg-13-6471-
707 2016
- 708 Dorrepaal E, Aerts R, Cornelissen JHC, Van Logtestijn RSP, Callaghan TV. 2006. Sphagnum modifies climate-
709 change impacts on subarctic vascular bog plants. *Functional Ecology* **20** : 31–41. DOI: 10.1111/j.1365-
710 2435.2006.01076.x
- 711 Driscoll WW. 2005. Divergent tree growth response to recent climatic warming, Lake Clark National Park and
712 Preserve, Alaska. *Geophysical Research Letters* **32** DOI: 10.1029/2005GL024258 [online] Available from:
713 <http://doi.wiley.com/10.1029/2005GL024258> (Accessed 29 May 2018)
- 714 Dullinger S, Dirnböck T, Grabherr G. 2003. Patterns of Shrub Invasion into High Mountain Grasslands of the
715 Northern Calcareous Alps, Austria. *Arctic, Antarctic, and Alpine Research* **35** : 434–441. DOI: 10.1657/1523-
716 0430(2003)035[0434:POSIII]2.0.CO;2

- 717 Durand Y, Giraud G, Laternser M, Etchevers P, Mérindol L, Lesaffre B. 2009a. Reanalysis of 47 Years of Climate
718 in the French Alps (1958–2005): Climatology and Trends for Snow Cover. *Journal of Applied Meteorology and*
719 *Climatology* **48** : 2487–2512. DOI: 10.1175/2009JAMC1810.1
- 720 Durand Y, Laternser M, Giraud G, Etchevers P, Lesaffre B, Mérindol L. 2009b. Reanalysis of 44 Yr of Climate in
721 the French Alps (1958–2002): Methodology, Model Validation, Climatology, and Trends for Air Temperature and
722 Precipitation. *Journal of Applied Meteorology and Climatology* **48** : 429–449. DOI: 10.1175/2008JAMC1808.1
- 723 Elmendorf SC et al. 2012. Plot-scale evidence of tundra vegetation change and links to recent summer warming.
724 *Nature Climate Change* **2** : 453–457. DOI: 10.1038/nclimate1465
- 725 Elmendorf SC et al. 2015. Experiment, monitoring, and gradient methods used to infer climate change effects on
726 plant communities yield consistent patterns. *Proceedings of the National Academy of Sciences* **112** : 448–452.
727 DOI: 10.1073/pnas.1410088112
- 728 Elsen PR, Tingley MW. 2015. Global mountain topography and the fate of montane species under climate change.
729 *Nature Climate Change* **5** : 772–776. DOI: 10.1038/nclimate2656
- 730 Ernakovich JG, Hopping KA, Berdanier AB, Simpson RT, Kachergis EJ, Steltzer H, Wallenstein MD. 2014.
731 Predicted responses of arctic and alpine ecosystems to altered seasonality under climate change. *Global Change*
732 *Biology* **20** : 3256–3269. DOI: 10.1111/gcb.12568
- 733 Escaravage N, Pornon A, Doche B, Till-Bottraud I. 1997. Breeding system in an alpine species: *Rhododendron*
734 *ferrugineum* L. (Ericaceae) in the French northern Alps. *Canadian Journal of Botany* **75** : 736–743. DOI:
735 10.1139/b97-084
- 736 Escaravage N, Questiau S, Pornon A, Doche B, Taberlet P. 1998. Clonal diversity in a *Rhododendron ferrugineum*
737 L.(Ericaceae) population inferred from AFLP markers. *Molecular ecology* **7** : 975–982.
- 738 Fajardo A, Piper FI. 2017. An assessment of carbon and nutrient limitations in the formation of the southern Andes
739 tree line. McGlone M (ed). *Journal of Ecology* **105** : 517–527. DOI: 10.1111/1365-2745.12697
- 740 Forbes BC, Fauria MM, Zetterberg P. 2010. Russian Arctic warming and ‘greening’ are closely tracked by tundra
741 shrub willows. *Global Change Biology* **16** : 1542–1554. DOI: 10.1111/j.1365-2486.2009.02047.x
- 742 Francon L, Corona C, Roussel E, Lopez Saez J, Stoffel M. 2017. Warm summers and moderate winter precipitation
743 boost *Rhododendron ferrugineum* L. growth in the Taillefer massif (French Alps). *Science of The Total*
744 *Environment* **586** : 1020–1031. DOI: 10.1016/j.scitotenv.2017.02.083
- 745 Franklin RS. 2013. Growth response of the alpine shrub, *Linanthus pungens*, to snowpack and temperature at a
746 rock glacier site in the eastern Sierra Nevada of California, USA. *Quaternary International* **310** : 20–33. DOI:
747 10.1016/j.quaint.2012.07.018
- 748 Fritts HC. 1976. *Tree rings and climate* . Academic Press: London ; New York
- 749 Gamm CM, Sullivan PF, Buchwal A, Dial RJ, Young AB, Watts DA, Cahoon SMP, Welker JM, Post E. 2018.
750 Declining growth of deciduous shrubs in the warming climate of continental western Greenland. Cornelissen H
751 (ed). *Journal of Ecology* **106** : 640–654. DOI: 10.1111/1365-2745.12882
- 752 Gerdol R, Siffi C, Iacumin P, Gualmini M, Tomaselli M. 2013. Advanced snowmelt affects vegetative growth and
753 sexual reproduction of *Vaccinium myrtillus* in a sub-alpine heath. Collins B (ed). *Journal of Vegetation Science*
754 **24** : 569–579. DOI: 10.1111/j.1654-1103.2012.01472.x
- 755 Gottfried M et al. 2012. Continent-wide response of mountain vegetation to climate change. *Nature Climate*
756 *Change* **2** : 111–115. DOI: 10.1038/nclimate1329
- 757 Grabherr G, Gottfried M, Pauli H. 1994. Climate effects on mountain plants. *Nature* **369** : 448–448. DOI:
758 10.1038/369448a0
- 759 Grace JB. 2006. *Structural equation modeling and natural systems* . Cambridge University Press: Cambridge, UK ;
760 New York
- 761 Gracia M, Montané F, Piqué J, Retana J. 2007. Overstory structure and topographic gradients determining diversity
762 and abundance of understory shrub species in temperate forests in central Pyrenees (NE Spain). *Forest Ecology*
763 *and Management* **242** : 391–397. DOI: 10.1016/j.foreco.2007.01.056
- 764 Hallinger M, Manthey M, Wilmking M. 2010. Establishing a missing link: warm summers and winter snow cover
765 promote shrub expansion into alpine tundra in Scandinavia. *New Phytologist* **186** : 890–899. DOI: 10.1111/j.1469-
766 8137.2010.03223.x

- 767 Hantel M, Ehrendorfer M, Haslinger A. 2000. Climate sensitivity of snow cover duration in Austria. *International*
768 *Journal of Climatology* **20** : 615–640. DOI: 10.1002/(SICI)1097-0088(200005)20:6<615::AID-
769 JOC489>3.0.CO;2-0
- 770 Hantel M, Maurer C, Mayer D. 2012. The snowline climate of the Alps 1961–2010. *Theoretical and Applied*
771 *Climatology* **110** : 517–537. DOI: 10.1007/s00704-012-0688-9
- 772 Hantemirov RM, Gorlanova LA, Shiyatov SG. 2000. Pathological tree-ring structures in Siberian juniper
773 (*Juniperus sibirica* Burgsd.) and their use for reconstructing extreme climatic events. *Russian Journal of Ecology*
774 **31** : 167–173. DOI: 10.1007/BF02762816
- 775 Hoch G. 2015. Carbon Reserves as Indicators for Carbon Limitation in Trees. In *Progress in Botany*, Lüttge U
776 and Beyschlag W (eds). Springer International Publishing: Cham; 321–346. [online] Available from:
777 http://link.springer.com/10.1007/978-3-319-08807-5_13 (Accessed 13 June 2018)
- 778 Hollesen J, Buchwal A, Rachlewicz G, Hansen BU, Hansen MO, Stecher O, Elberling B. 2015. Winter warming
779 as an important co-driver for *Betula nana* growth in western Greenland during the past century. *Global Change*
780 *Biology* **21** : 2410–2423. DOI: 10.1111/gcb.12913
- 781 Holmes RL. 1994. *Dendrochronology Program Library User's Manual*. Laboratory of Tree-Ring Research,
782 University of Arizona: Tucson, Arizona
- 783 Inouye DW. 2000. The ecological and evolutionary significance of frost in the context of climate change. *Ecology*
784 *Letters* **3** : 457–463. DOI: 10.1046/j.1461-0248.2000.00165.x
- 785 Jochner M, Bugmann H, Nötzli M, Bigler C. 2018. Tree growth responses to changing temperatures across space
786 and time: a fine-scale analysis at the treeline in the Swiss Alps. *Trees* **32** : 645–660. DOI: 10.1007/s00468-017-
787 1648-x
- 788 Jonas T, Rixen C, Sturm M, Stoeckli V. 2008. How alpine plant growth is linked to snow cover and climate
789 variability. *Journal of Geophysical Research* **113** DOI: 10.1029/2007JG000680 [online] Available from:
790 <http://doi.wiley.com/10.1029/2007JG000680> (Accessed 12 June 2018)
- 791 Kline RB. 2011. *Principles and practice of structural equation modeling*. 3rd ed. Guilford Press: New York
- 792 Kolishchuk V. 1990. Dendroclimatological study of prostrate woody plant. In *Methods of Dendrochronology,*
793 *Applications in the Environmental Sciences*, . Springer Netherlands: Dordrecht; 51–55.
- 794 Körner C. 2003. *Alpine plant life: functional plant ecology of high mountain ecosystems*. 2nd ed. Springer: Berlin ;
795 New York
- 796 Kudo G, Suzuki S. 1999. Flowering phenology of alpine plant communities along a gradient of snowmelt timing.
797 *Polar Bioscience* **12** : 100–113.
- 798 Lafaysse M, Morin S, Coléou C, Vernay M, Serça D, Besson F, Willemet J-M, Giraud G, Durand Y. 2013.
799 Towards a new chain of models for avalanche hazard forecasting in French mountain ranges, including low
800 altitude mountains. presented at the International Snow Science Workshop. Grenoble - Chamonix Mont Blanc.
801 162–166 pp.
- 802 Larcher W, Siegwolf R. 1985. Development of acute frost drought in *Rhododendron ferrugineum* at the alpine
803 timberline. *Oecologia* **67** : 298–300. DOI: 10.1007/BF00384304
- 804 Lenoir J, Gegout JC, Marquet PA, de Ruffray P, Brisse H. 2008. A Significant Upward Shift in Plant Species
805 Optimum Elevation During the 20th Century. *Science* **320** : 1768–1771. DOI: 10.1126/science.1156831
- 806 Liang E, Eckstein D. 2009. Dendrochronological potential of the alpine shrub *Rhododendron nivale* on the south-
807 eastern Tibetan Plateau. *Annals of Botany* **104** : 665–670. DOI: 10.1093/aob/mcp158
- 808 Liang E, Lu X, Ren P, Li X, Zhu L, Eckstein D. 2012. Annual increments of juniper dwarf shrubs above the tree
809 line on the central Tibetan Plateau: a useful climatic proxy. *Annals of Botany* **109** : 721–728. DOI:
810 10.1093/aob/mcr315
- 811 Liston GE, Mcfadden JP, Sturm M, Pielke RA. 2002. Modelled changes in arctic tundra snow, energy and moisture
812 fluxes due to increased shrubs. *Global Change Biology* **8** : 17–32. DOI: 10.1046/j.1354-1013.2001.00416.x
- 813 López-Moreno JJ. 2005. Recent Variations of Snowpack Depth in the Central Spanish Pyrenees. *Arctic, Antarctic,*
814 *and Alpine Research* **37** : 253–260. DOI: 10.1657/1523-0430(2005)037[0253:RVOSDI]2.0.CO;2

- 815 Lu X, Camarero JJ, Wang Y, Liang E, Eckstein D. 2015. Up to 400-year-old *Rhododendron* shrubs on the
816 southeastern Tibetan Plateau: prospects for shrub-based dendrochronology. *Boreas* **44** : 760–768. DOI:
817 10.1111/bor.12122
- 818 Madrigal-González J, Andivia E, Zavala MA, Stoffel M, Calatayud J, Sánchez-Salguero R, Ballesteros-Cánovas
819 J. 2018. Disentangling the relative role of climate change on tree growth in an extreme Mediterranean environment.
820 *Science of The Total Environment* **642** : 619–628. DOI: 10.1016/j.scitotenv.2018.06.064
- 821 Madrigal-González J, Ballesteros-Cánovas JA, Herrero A, Ruiz-Benito P, Stoffel M, Lucas-Borja ME, Andivia E,
822 Sancho-García C, Zavala MA. 2017. Forest productivity in southwestern Europe is controlled by coupled North
823 Atlantic and Atlantic Multidecadal Oscillations. *Nature Communications* **8** DOI: 10.1038/s41467-017-02319-0
824 [online] Available from: <http://www.nature.com/articles/s41467-017-02319-0> (Accessed 16 August 2019)
- 825 Malfasi F, Cannone N. 2020. Climate Warming Persistence Triggered Tree Ingression After Shrub Encroachment
826 in a High Alpine Tundra. *Ecosystems* DOI: 10.1007/s10021-020-00495-7 [online] Available from:
827 <http://link.springer.com/10.1007/s10021-020-00495-7> (Accessed 24 February 2020)
- 828 Marty C, Schlögl S, Bavay M, Lehning M. 2017. How much can we save? Impact of different emission scenarios
829 on future snow cover in the Alps. *The Cryosphere* **11** : 517–529. DOI: 10.5194/tc-11-517-2017
- 830 Mitchell RJ. 1992. Testing Evolutionary and Ecological Hypotheses Using Path Analysis and Structural Equation
831 Modelling. *Functional Ecology* **6** : 123. DOI: 10.2307/2389745
- 832 Molau U, Nordenhall U, Eriksen B. 2005. Onset of flowering and climate variability in an alpine landscape: a 10-
833 year study from Swedish Lapland. *American Journal of Botany* **92** : 422–431. DOI: 10.3732/ajb.92.3.422
- 834 Mote PW, Hamlet AF, Clark MP, Lettenmaier DP. 2005. DECLINING MOUNTAIN SNOWPACK IN
835 WESTERN NORTH AMERICA*. *Bulletin of the American Meteorological Society* **86** : 39–50. DOI:
836 10.1175/BAMS-86-1-39
- 837 Myers-Smith IH et al. 2011. Shrub expansion in tundra ecosystems: dynamics, impacts and research priorities.
838 *Environmental Research Letters* **6** : 045509. DOI: 10.1088/1748-9326/6/4/045509
- 839 Myers-Smith IH et al. 2015a. Climate sensitivity of shrub growth across the tundra biome. *Nature Climate Change*
840 **5** : 887–891. DOI: 10.1038/nclimate2697
- 841 Myers-Smith IH et al. 2015b. Methods for measuring arctic and alpine shrub growth: A review. *Earth-Science*
842 *Reviews* **140** : 1–13. DOI: 10.1016/j.earscirev.2014.10.004
- 843 Myers-Smith IH et al. 2019. Eighteen years of ecological monitoring reveals multiple lines of evidence for tundra
844 vegetation change. *Ecological Monographs* **89** : e01351. DOI: 10.1002/ecm.1351
- 845 Myers-Smith IH et al. 2020. Complexity revealed in the greening of the Arctic. *Nature Climate Change* **10** : 106–
846 117. DOI: 10.1038/s41558-019-0688-1
- 847 Neuner G, Ambach D, Aichner K. 1999. Impact of snow cover on photoinhibition and winter desiccation in
848 evergreen *Rhododendron ferrugineum* leaves during subalpine winter. *Tree Physiology* **19** : 725–732. DOI:
849 10.1093/treephys/19.11.725
- 850 Niittynen P, Heikkinen RK, Luoto M. 2018. Snow cover is a neglected driver of Arctic biodiversity loss. *Nature*
851 *Climate Change* **8** : 997–1001. DOI: 10.1038/s41558-018-0311-x
- 852 Ozenda PG. 1985. La végétation de la chaîne alpine: dans l'espace montagnard européen . Masson: Paris u.a
- 853 Parmesan C, Yohe G. 2003. A globally coherent fingerprint of climate change impacts across natural systems.
854 *Nature* **421** : 37–42. DOI: 10.1038/nature01286
- 855 Pautou G, Cadel G, Girel J. 1992. Le bassin de Bourd d'Oisans, carrefour phytogéographique des Alpes. *Revue*
856 *d'Ecologie Alpine* : 23–43.
- 857 Pearson RG, Phillips SJ, Loranty MM, Beck PSA, Damoulas T, Knight SJ, Goetz SJ. 2013. Shifts in Arctic
858 vegetation and associated feedbacks under climate change. *Nature Climate Change* **3** : 673–677. DOI:
859 10.1038/nclimate1858
- 860 Pellizzari E, Camarero JJ, Gazol A, Sangüesa-Barreda G, Carrer M. 2016. Wood anatomy and carbon-isotope
861 discrimination support long-term hydraulic deterioration as a major cause of drought-induced dieback. *Global*
862 *Change Biology* **22** : 2125–2137. DOI: 10.1111/gcb.13227

863 Pellizzari E, Pividori M, Carrer M. 2014. Winter precipitation effect in a mid-latitude temperature-limited
864 environment: the case of common juniper at high elevation in the Alps. *Environmental Research Letters* **9** : 104021.
865 DOI: 10.1088/1748-9326/9/10/104021

866 Pérez-de-Lis G, García-González I, Rozas V, Olano JM. 2016. Feedbacks between earlywood anatomy and non-
867 structural carbohydrates affect spring phenology and wood production in ring-porous oaks. *Biogeosciences* **13** :
868 5499–5510. DOI: 10.5194/bg-13-5499-2016

869 Phoenix GK, Bjerke JW. 2016. Arctic browning: extreme events and trends reversing arctic greening. *Global*
870 *Change Biology* **22** : 2960–2962. DOI: 10.1111/gcb.13261

871 Pornon A, Doche B. 1995. Influence des populations de *Rhododendron ferrugineum* L. sur la végétation subalpine
872 (Alpes du Nord-France). *Feddes Repertorium* **106** : 179–191. DOI: 10.1002/fedr.19951060312

873 Pornon A, Doche B. 1996. Age structure and dynamics of *Rhododendron ferrugineum* L. populations in the
874 northwestern French Alps. *Journal of Vegetation Science* **7** : 265–272.

875 Pornon A, Escaravage N, Till-Bottraud I. 1997. Variation of reproductive traits in *Rhododendron ferrugineum* L.
876 (Ericaceae) populations along a successional gradient. *Plant Ecology* : 1–11.

877 R Core Team. 2016. R: A Language and Environment for Statistical Computing. R Foundation for Statistical
878 Computing . R Foundation for Statistical Computing: Vienna, Austria [online] Available from: [http://www.R-](http://www.R-project.org/)
879 [project.org/](http://www.R-project.org/)

880 Reid PC et al. 2016. Global impacts of the 1980s regime shift. *Global Change Biology* **22** : 682–703. DOI:
881 10.1111/gcb.13106

882 Rixen C, Dawes MA, Wipf S, Hagedorn F. 2012. Evidence of enhanced freezing damage in treeline plants during
883 six years of CO₂ enrichment and soil warming. *Oikos* **121** : 1532–1543. DOI: 10.1111/j.1600-0706.2011.20031.x

884 Rixen C, Schwoerer C, Wipf S. 2010. Winter climate change at different temporal scales in *Vaccinium myrtillus* ,
885 an Arctic and alpine dwarf shrub. *Polar Research* **29** : 85–94. DOI: 10.1111/j.1751-8369.2010.00155.x

886 Ropars P, Lévesque E, Boudreau S. 2015. How do climate and topography influence the greening of the forest
887 tundra ecotone in northern Québec? A dendrochronological analysis of *Betula glandulosa*. *Journal of Ecology* :
888 n/a-n/a. DOI: 10.1111/1365-2745.12394

889 Rosseel Y. 2012. **lavaan** : An R Package for Structural Equation Modeling. *Journal of Statistical Software* **48** DOI:
890 10.18637/jss.v048.i02 [online] Available from: <http://www.jstatsoft.org/v48/i02/> (Accessed 26 July 2019)

891 Schmidt NM, Baittinger C, Kollmann J, Forchhammer MC. 2010. Consistent Dendrochronological Response of
892 the Dioecious *Salix arctica* to Variation in Local Snow Precipitation across Gender and Vegetation Types. *Arctic,*
893 *Antarctic, and Alpine Research* **42** : 471–475. DOI: 10.1657/1938-4246-42.4.471

894 Schweingruber FH, Börner A, Schulze E-D. 2011. Atlas of Stem Anatomy in Herbs, Shrubs and Trees . Springer
895 Berlin Heidelberg: Berlin, Heidelberg

896 Steger C, Kotlarski S, Jonas T, Schär C. 2013. Alpine snow cover in a changing climate: a regional climate model
897 perspective. *Climate Dynamics* **41** : 735–754. DOI: 10.1007/s00382-012-1545-3

898 Steinbauer MJ et al. 2018. Accelerated increase in plant species richness on mountain summits is linked to
899 warming. *Nature* **556** : 231–234. DOI: 10.1038/s41586-018-0005-6

900 Stinson KA. 2005. Effects of Snowmelt Timing and Neighbor Density on the Altitudinal Distribution of *Potentilla*
901 *diversifolia* in Western Colorado, U.S.A. *Arctic, Antarctic, and Alpine Research* **37** : 379–386. DOI:
902 10.1657/1523-0430(2005)037[0379:EOSTAN]2.0.CO;2

903 Stocker TF, Qin GK, Plattner M. 2013. Climate Change 2013: The Physical Science Basis. Contribution of
904 Working Group I to the Fifth Assessment Report of the Intergovernmental Panel on Climate Change . Cambridge
905 University Press

906 Sturm M, Holmgren J, McFadden JP, Liston GE, Chapin FS, Racine CH. 2001. Snow–Shrub Interactions in Arctic
907 Tundra: A Hypothesis with Climatic Implications. *Journal of Climate* **14** : 336–344. DOI: 10.1175/1520-
908 0442(2001)014<0336:SSIIAT>2.0.CO;2

909 Tape K, Sturm M, Racine C. 2006. The evidence for shrub expansion in Northern Alaska and the Pan-Arctic.
910 *Global Change Biology* **12** : 686–702. DOI: 10.1111/j.1365-2486.2006.01128.x

911 Treharne R, Bjerke JW, Tømmervik H, Stendardi L, Phoenix GK. 2019. Arctic browning: Impacts of extreme
912 climatic events on heathland ecosystem CO₂ fluxes. *Global Change Biology* **25** : 489–503. DOI:
913 10.1111/gcb.14500

914 Vaganov EA, Hughes MK, Kiryanov AV, Schweingruber FH, Silkin PP. 1999. Influence of snowfall and melt
915 timing on tree growth in subarctic Eurasia. *Nature* **400** : 149–151.

916 Verfaillie D, Lafaysse M, Déqué M, Eckert N, Lejeune Y, Morin S. 2018. Multi-component ensembles of future
917 meteorological and natural snow conditions for 1500 m altitude in the Chartreuse mountain range, Northern French
918 Alps. *The Cryosphere* **12** : 1249–1271. DOI: 10.5194/tc-12-1249-2018

919 Vionnet V, Brun E, Morin S, Boone A, Faroux S, Le Moigne P, Martin E, Willemet J-M. 2012. The detailed
920 snowpack scheme Crocus and its implementation in SURFEX v7.2. *Geoscientific Model Development* **5** : 773–
921 791. DOI: 10.5194/gmd-5-773-2012

922 Walther G-R, Post E, Convey P, Menzel A, Parmesan C, Beebee TJC, Fromentin J-M, Hoegh-Guldberg O, Bairlein
923 F. 2002. Ecological responses to recent climate change. *Nature* **416** : 389–395. DOI: 10.1038/416389a

924 Weijers S, Beckers N, Löffler J. 2018a. Recent spring warming limits near-treeline deciduous and evergreen alpine
925 dwarf shrub growth. *Ecosphere* **9** : e02328. DOI: 10.1002/ecs2.2328

926 Weijers S, Broekman R, Rozema J. 2010. Dendrochronology in the High Arctic: July air temperatures
927 reconstructed from annual shoot length growth of the circumpolar dwarf shrub *Cassiope tetragona*. *Quaternary*
928 *Science Reviews* **29** : 3831–3842. DOI: 10.1016/j.quascirev.2010.09.003

929 Weijers S, Pape R, Löffler J, Myers-Smith IH. 2018b. Contrasting shrub species respond to early summer
930 temperatures leading to correspondence of shrub growth patterns. *Environmental Research Letters* **13** : 034005.
931 DOI: 10.1088/1748-9326/aaa5b8

932 Wheeler JA, Cortés AJ, Sedlacek J, Karrenberg S, van Kleunen M, Wipf S, Hoch G, Bossdorf O, Rixen C. 2016.
933 The snow and the willows: earlier spring snowmelt reduces performance in the low-lying alpine shrub *Salix*
934 *herbacea*. Cornelissen H (ed). *Journal of Ecology* **104** : 1041–1050. DOI: 10.1111/1365-2745.12579

935 Wilmking M. 2005. Increased temperature sensitivity and divergent growth trends in circumpolar boreal forests.
936 *Geophysical Research Letters* **32** DOI: 10.1029/2005GL023331 [online] Available from:
937 <http://doi.wiley.com/10.1029/2005GL023331> (Accessed 29 May 2018)

938 Wilmking M et al. 2020. Global assessment of relationships between climate and tree growth. *Global Change*
939 *Biology* : gcb.15057. DOI: 10.1111/gcb.15057

940 Wipf S. 2010. Phenology, growth, and fecundity of eight subarctic tundra species in response to snowmelt
941 manipulations. *Plant Ecology* **207** : 53–66. DOI: 10.1007/s11258-009-9653-9

942 Wipf S, Rixen C. 2010. A review of snow manipulation experiments in Arctic and alpine tundra ecosystems. *Polar*
943 *Research* **29** : 95–109. DOI: 10.1111/j.1751-8369.2010.00153.x

944 Wipf S, Rixen C, Mulder CPH. 2006. Advanced snowmelt causes shift towards positive neighbour interactions in
945 a subarctic tundra community. *Global Change Biology* **12** : 1496–1506. DOI: 10.1111/j.1365-2486.2006.01185.x

946 Wipf S, Stoeckli V, Bebi P. 2009. Winter climate change in alpine tundra: plant responses to changes in snow
947 depth and snowmelt timing. *Climatic Change* **94** : 105–121. DOI: 10.1007/s10584-009-9546-x

948 Young AB, Watts DA, Taylor AH, Post E. 2016. Species and site differences influence climate-shrub growth
949 responses in West Greenland. *Dendrochronologia* **37** : 69–78. DOI: 10.1016/j.dendro.2015.12.007

950 Zalatan R, Gajewski K. 2006. Dendrochronological Potential of *Salix alaxensis* from the Kuujua River Area,
951 Western Canadian Arctic. *Tree-Ring Research* **62** : 75–82. DOI: 10.3959/1536-1098-62.2.75

952 Zang C, Biondi F. 2015. treeclim: an R package for the numerical calibration of proxy-climate relationships.
953 *Ecography* **38** : 431–436. DOI: 10.1111/ecog.01335

954 Zuur AF, Ieno EN, Elphick CS. 2010. A protocol for data exploration to avoid common statistical problems: Data
955 exploration. *Methods in Ecology and Evolution* **1** : 3–14. DOI: 10.1111/j.2041-210X.2009.00001.x

956

957

958